

We have reported previously that HCV core protein specifically interacts with a proteasome activator PA28 γ /REG γ in the nucleus and is digested by a PA28 γ -dependent proteasome activity.⁷ *In vivo* experiments in a mouse model suggest that PA28 γ plays a critical role in the pathogenesis induced by HCV core protein.^{8,9} PA28 γ forms a homoheptamer in the nucleus and enhances the proteasome-mediated cleavage after basic amino acid residues, whereas PA28 α and PA28 β exhibit 41% and 34% homology to PA28 γ , respectively, and form a heteroheptamer in the cytoplasm to activate cleavage after hydrophobic, acidic, or basic amino acid residues.¹⁰ Recently, several groups reported that PA28 γ interacts with steroid receptor coactivator-3 and cell cycle suppressors such as p21^{WAF1/CIP1}, p16^{INK4A}, and p19^{ARF}, and enhances the degradation of these proteins in a ubiquitin- and adenosine triphosphate-independent manner.¹¹⁻¹³ Furthermore, other mechanisms of ubiquitin-independent degradation have been considered for cell cycle regulation, summarized in the review of Jariel-Encontre et al.¹⁴ However, the precise physiological functions of PA28 γ are largely unknown *in vivo*, because PA28 γ -knockout mice exhibit only mild growth retardation and live approximately as long as their control littermates.^{15,16}

HCV core protein is degraded in a PA28 γ -dependent and ubiquitin-independent manner in the nucleus,^{7,17} while E6AP is also involved in the degradation of the core protein in a ubiquitin-dependent manner.^{17,18} E6AP is a member of E3 ligases, which catalyze ubiquitin ligation of host and foreign proteins. Knockdown of E6AP suppressed degradation of HCV core protein and enhanced the release of infectious particles, suggesting that E6AP negatively regulates HCV propagation.¹⁸ However, the role of PA28 γ in the propagation of HCV has not yet been characterized. In this study, we examined the biological significance of PA28 γ in the propagation of HCV.

Materials and Methods

Transfection, Immunoblotting, and RNA Interference. Plasmid DNA was transfected into Huh7OK1 cells by way of liposome-mediated transfection using Lipofectamine LTX with Plus reagent (Invitrogen, Carlsbad, CA). Expression of HCV core protein was determined by way of enzyme-linked immunosorbent assay as described.¹⁹ Immunoblotting was performed as described.⁸ The small interfering RNAs (siRNAs) targeted to the PA28 γ gene were purchased from

Ambion (Austin, TX) and were introduced into the cell lines using Lipofectamine RNAiMax (Invitrogen). siRNAs with the Ambion siRNA ID numbers 138669 and 138670 were designated as siPA28 γ 1 and siPA28 γ 2, respectively. Antibodies and plasmids are described in the Supporting Information.

Cell Lines and Virus Infection. All cell lines were cultured at 37°C under the conditions of humidified atmosphere and 5% CO₂. The human hepatoma cell line Huh7OK1 and derivative cell lines were maintained in Dulbecco's modified Eagle's medium (Sigma, St. Louis, MO) supplemented with nonessential amino acids, sodium pyruvate, and 10% fetal bovine serum. The Huh7-derived cell line harboring a subgenomic or a full-length HCV replicon RNA²⁰ was maintained in Dulbecco's modified Eagle's medium containing 10% fetal bovine serum, nonessential amino acids, sodium pyruvate, and 1 mg/mL G418 (Nakarai Tesque, Kyoto, Japan). Huh7OK1 cells were transfected with pSilencer-shPA28 γ 4 or a control plasmid, pSilencer 2.1 U6 hygro negative control (Ambion), and drug-resistant clones were selected by treatment with hygromycin (Wako, Tokyo, Japan) at a final concentration of 100 μ g/mL. Huh7OK1 cells transfected with the control plasmid were selected with puromycin and designated as shCntrl, whereas those transfected with pSilencer-shPA28 γ 4 were established by limited dilution,⁸ and two of the resulting cell lines were designated as KD5 and KD7. Plasmids encoding wild-type or mutant PA28 γ complementary DNAs resistant to siRNA against PA28 γ were prepared by using the silent mutations as reported.⁸ These plasmids were transfected into Huh7OK1 cells and cultivated in medium containing 0.1 μ g/mL of puromycin for 2 days. The surviving cells were used for virus infection. The shCtrl and KD5 cells were transformed with pSilencer shE6AP or pSilencer 3.1 H1 puro negative control (Ambion) and treated with 0.1 μ g/mL of puromycin for 2 days. The surviving cells were infected with JFH-1 virus at a multiplicity of infection (moi) of 0.05. The viral RNA derived from the plasmid pJFH1 was transcribed and introduced into Huh7OK1 cells according to the method of Wakita et al.²¹ The infectivity of JFH1 strain was determined using a focus-forming assay²¹ and is expressed in focus-forming units. The Huh7 cell line harboring subgenomic replicon RNA of the Con1 or JFH1 strain was prepared according to the method of Pietschmann et al.²² The infectivity of the Japanese encephalitis virus (JEV) was determined by an immunostaining focus assay as described²³ and is expressed in focus-forming units. Colony formation and replication assays, quantitative

reverse-transcription polymerase chain reaction, and estimation of cell growth was performed as described in the Supporting Information.

Immunofluorescent Staining. Huh7OK1-derived cells were seeded at 0.5×10^4 cells/well in an eight-well chamber slide, infected with JFH-1 virus at an moi of 0.3 after incubation at 37°C for 24 hours, stained with Bodipy 558/568 C₁₂ according to the method of Targett-Adams et al.²⁴ at 4 days postinfection, and then fixed at 4°C for 30 minutes with 4% paraformaldehyde in phosphate-buffered saline. After treatment of cells with 1 μg/mL of RNase A, nuclei were stained with 50 μM Hoechst 33258. The fixed cells were permeabilized with 20 mM Tris-HCl containing 1% Nonidet P-40 and 135 mM NaCl at room temperature for 5 minutes, reacted with rabbit anti-core or anti-NS5A antibody followed by Alexa Fluor 488-goat antibody to rabbit immunoglobulin G, washed three times with phosphate-buffered saline, and observed with a FluoView FV1000 laser scanning confocal microscope (Olympus, Tokyo, Japan). The percentage of the area occupied by the core protein in nucleus and cytoplasm was calculated using Image-Pro software (Media Cybernetics). The percentage of the nuclear core protein to the total core protein was examined randomly in 10 fields of every three wells. The percentage of the nuclear NS5A to total NS5A was estimated by the same method as the ratio of the core protein.

Results

Transient Knockdown of PA28γ Prior to or After Infection With HCV Reduces Particle Production. We reported previously that Huh7OK1 cells are as permissive to JFH-1 virus infection as Huh7.5.1 cells.²⁵ The Huh-7OK1 cell line retained the ability to produce type I IFNs through the RIG-I-dependent signaling pathway upon infection with RNA viruses and exhibited a cell surface expression level of human CD81 comparable to that of the parental cell line. However, the mechanism through which the Huh7OK1 cell line exhibits highly permissive to JFH-1 virus infection has not been clarified yet. Two siRNAs were used to knock down PA28γ, but only one, siPA28γ1, was used because the other had off-target effects (Supporting Fig. 1). To examine the effect of PA28γ on the propagation of HCV, siPA28γ1 was introduced into Huh7OK1 cells 24 hours before infection. The levels of viral RNA, core protein, and infectious viral titer were determined at 48 and 96 hours postinfection. Viral RNA in the culture supernatant and cells was clearly reduced by the knockdown of

PA28γ at 48 and 96 hours postinfection, respectively (Fig. 1A), whereas a significant reduction of core protein expression was detected at 96 hours but not at 48

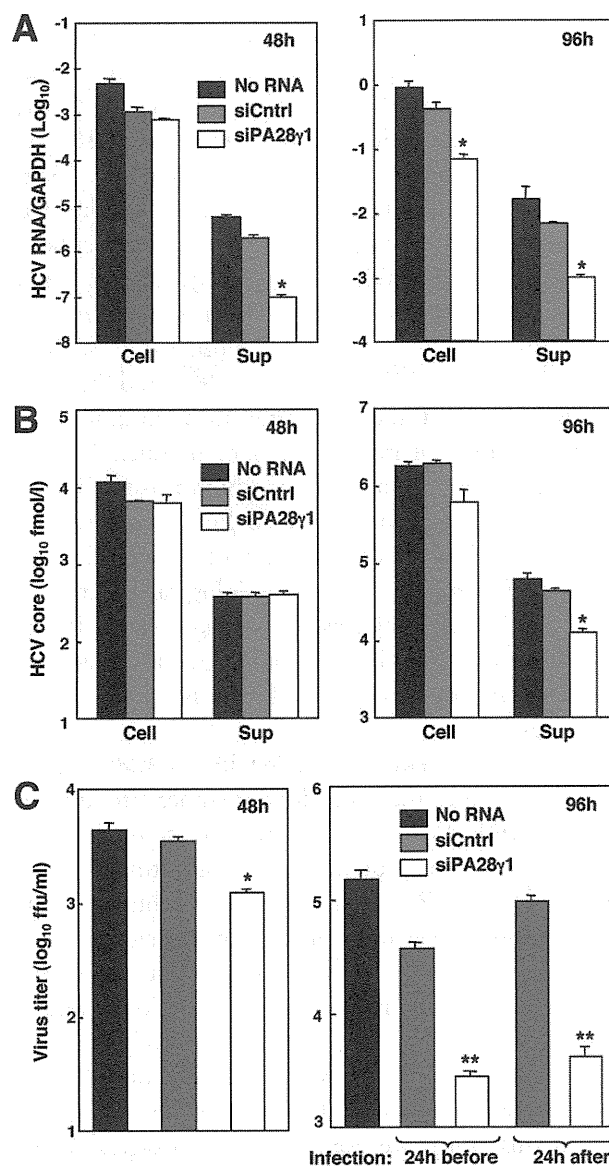


Fig. 1. Transient knockdown of PA28γ before or after infection with HCV reduces particle production. (A) Huh7OK1 cells transfected with a control siRNA (siCntrl) or PA28γ siRNA1 were infected with JFH-1 virus at 24 hours posttransfection and then harvested at 48 hours (left panel) and 96 hours postinfection (right panel). The quantity of HCV RNA in cells and supernatants was determined by way of quantitative reverse-transcription polymerase chain reaction. (B) The expression of HCV core protein in cells and supernatants at 48 hours (left panel) and 96 hours (right panel) postinfection was determined by ELISA. (C) Huh7OK1 cells that were transfected with siCntrl or PA28γ siRNA1 were infected with JFH-1 virus at 24 hours posttransfection. The infectivity of the virus in the culture supernatant was determined by a focus-forming assay at 48 hours postinfection (left panel). Those transfected with the siRNAs at 24 hours before and after infection with JFH-1 virus were determined similarly at 96 hours postinfection (right panel). * $P < 0.05$, ** $P < 0.01$ versus control siRNA-transfected cells. Data are representative of three independent experiments.

hours postinfection (Fig. 1B). Infectious viral titer in the culture supernatant was significantly reduced at 48 and 96 hours postinfection by the PA28 γ knockdown (Fig. 1C), consistent with the suppression of the viral RNA in the supernatant. Furthermore, a comparable suppression of the production of infectious particles in the supernatant was also achieved by introducing siPA28 γ 1 into cells even at 24 hours postinfection (Fig. 1C, right panel). These results suggest that PA28 γ participates in the regulation of HCV propagation in postentry steps.

Stable Knockdown of PA28 γ Impairs Viral Propagation. To establish the PA28 γ knockdown cell lines, Huh7OK1 cells were transfected with a plasmid encoding a short hairpin RNA (shRNA) targeted to PA28 γ and selected with hygromycin, resulting in two clones—KD5 and KD7—that exhibited a clear reduction of PA28 γ expression (Fig. 2A). Although the suppression of PA28 γ expression in KD7 cells was slightly more efficient than that in KD5 cells, the growth of KD7 cells was impaired (Fig. 2B). Viral production in the culture supernatants in cells infected with the JFH-1 virus was significantly impaired in PA28 γ knockdown KD5 cells compared with control cells (Fig. 2C). The viral RNA and core protein in the supernatant were also reduced in KD5 cells (Fig. 2D). Expression of siRNA-resistant PA28 γ in PA28 γ knockdown KD5 and KD7 cells recovered virus production in the supernatant to a level similar to that in the control cells transfected with an empty vector, and overexpression of siRNA-resistant PA28 γ in control cells slightly enhanced virus production (Fig. 2E). Our previous data suggest that capsid protein of JEV does not bind to PA28 γ .⁷ To examine whether PA28 γ regulates JEV propagation, KD5 and shCntrl cells were infected with JEV at an moi of 0.5. The infectivity of JEV in KD5 cells was similar to that in shCntrl cells (Fig. 2F), suggesting that PA28 γ does not participate in the virus production pathway of JEV. These results further support the notion that PA28 γ participates in HCV propagation.

Knockdown of PA28 γ Exhibits No Effect on Viral RNA Replication. Although knockdown of PA28 γ resulted in the suppression of viral particle and RNA production in the culture supernatant at 48 hours postinfection with JHF-1 virus, viral RNA in the cells was not reduced (Fig. 1), suggesting that PA28 γ does not participate in viral replication. To gain more insight on this point, we examined the effect of PA28 γ knockdown on RNA replication in replicon cells. Transient knockdown of PA28 γ through introduction of siPA28 γ into the subgenomic HCV replicon cells

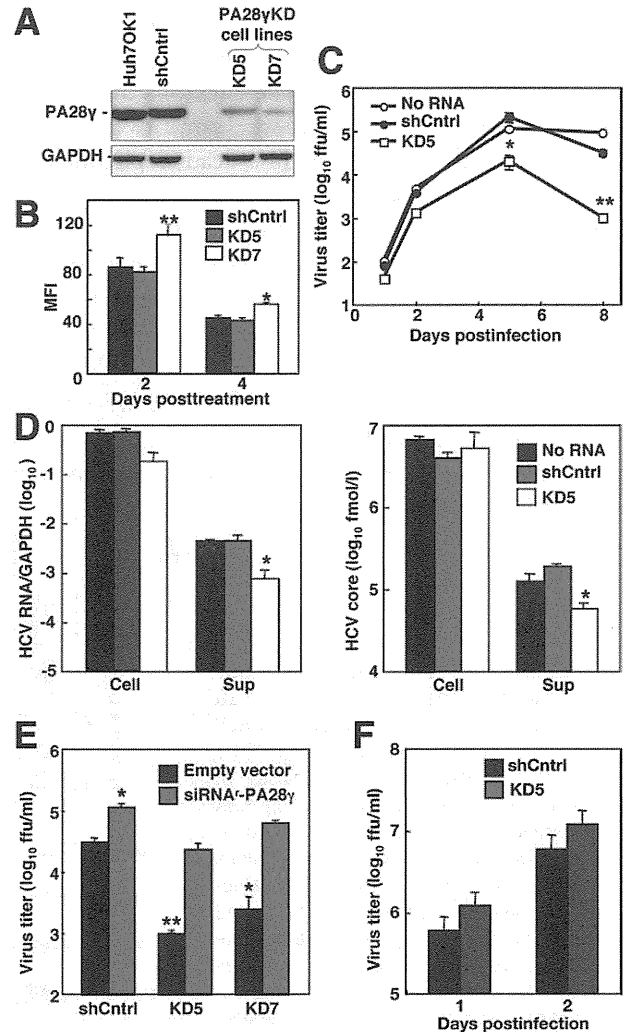


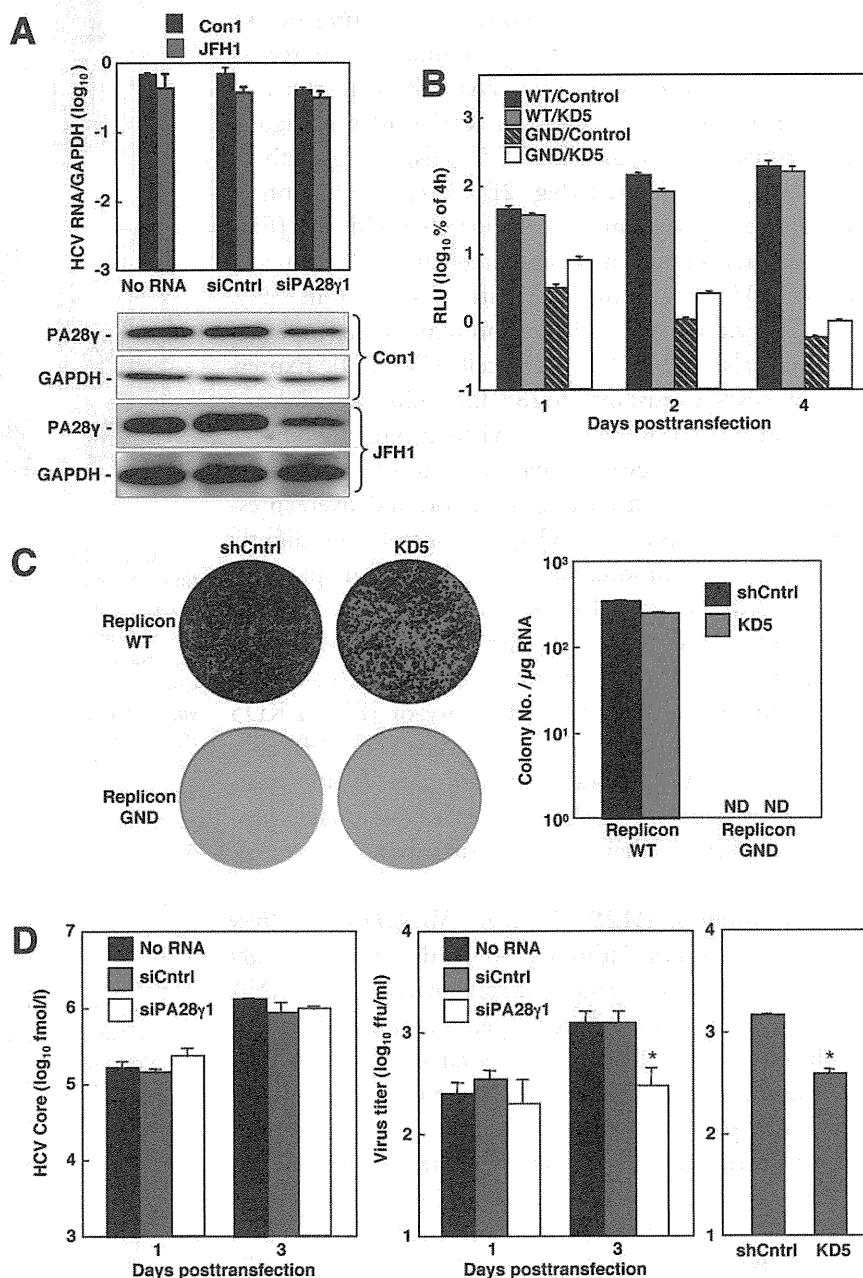
Fig. 2. Establishment of PA28 γ knockdown cell lines and propagation of HCV. (A) Huh7OK1 cells were transfected with pSilencer shPA28 γ or control plasmid and selected by hygromycin at 48 hours posttransfection. Two PA28 γ knockdown cell lines (KD5 and KD7) and one control cell line (shCntrl) were established, and PA28 γ knockdown was confirmed by way of immunoblotting. (B) Growth of the cell lines was determined by staining with carboxyfluorescein succinimidyl ester. (C,D) KD5 and shCntrl cell lines were infected with the JFH-1 virus at an moi of 0.05. The infectious virus titers in the culture supernatants (C) was determined by way of focus-forming assay. The virus RNA (D, left panel) and the core protein (D, right panel) in both cell and the supernatant were determined at 5 days postinfection by way of ELISA and quantitative reverse-transcription polymerase chain reaction, respectively. (E) The plasmid encoding an siRNA-resistant PA28 γ or empty vector was transfected into the cell lines, seeded at 5×10^4 cells into a six-well plate after cultivation in the presence of puromycin for 2 days, and infected with JFH-1 virus at an moi of 0.05. The viral titers were determined at 5 days postinfection. * $P < 0.05$, ** $P < 0.01$ versus shCntrl cells transfected with an empty vector. (F) KD5 and shCntrl cell lines were infected with the JEV virus at an moi of 0.5. The infectivity of JEV in the supernatant was determined at 1 and 2 days postinfection. Data are representative of three independent experiments.

derived from the Con1 or JFH-1 strain induced no significant reduction of HCV RNA (Fig. 3A). Furthermore, luciferase activities in the stable PA28 γ

knockdown cell line KD5 and the control cell line transfected with the subgenomic replicon RNA (WT) were gradually increased until 4 days posttransfection, whereas luciferase activities in the same two cell lines transfected with the polymerase-dead replicon RNA (GND) were decreased in a time-dependent manner (Fig. 3B). Next, to explore the effect of PA28 γ knockdown on the viral replication over a longer period, replicon RNA encoding the neomycin-resistance gene was transfected into the cell lines for a colony formation assay. The numbers of colonies in the KD5 cell line after 4 weeks of selection with G418 were similar to those in the control cell line (Fig. 3C). To further clarify the roles of PA28 γ on the postreplication steps,

in vitro transcribed full-length viral RNA was transfected into Huh7OK1 cells, and siPA28 γ 1 was then introduced into the cells at 24 hours posttransfection of viral RNA. Intracellular core protein was increased in a time-dependent manner, but no significant difference was observed between cells transfected with control siRNA and those transfected with siPA28 γ 1 (Fig. 3D, left panel). However, infectious virus titers in the supernatant were significantly decreased by the transient and stable knockdown of PA28 γ compared with control cells (Fig. 3D, middle and right panels). Furthermore, PA28 γ did not contribute to the virus production of JEV (Fig. 2F), suggesting that the general sorting pathway of the flavivirus is functional under

Fig. 3. Effect of PA28 γ knockdown on HCV RNA replication. (A) The siCntrl or siPA28 γ 1 (10 nM) was transfected into the subgenomic HCV replicon cells derived from Con1 and JFH-1 strains. The transfected cells were harvested at 72 hours posttransfection. The replicon RNA was determined by quantitative reverse-transcription polymerase chain reaction at 72 hours posttransfection (upper). PA28 γ or glyceraldehyde 3-phosphate dehydrogenase was detected by way of immunoblotting. Cell lysates were subjected to western blotting using antibodies to PA28 γ and glyceraldehyde 3-phosphate dehydrogenase (lower). (B) The HCV replicon RNA encoding luciferase gene (WT) or the HCV replicon RNA that has a replication-deficient mutation (GND) was transfected into the shCntrl (Control) and KD5 cell lines. Relative luciferase activity was determined using the activity at 4 hours post-electroporation as a transfection efficiency. (C) Colony formation assay. Replicon RNA encoding the neomycin-resistance gene was transfected into the shCntrl and KD5 cell lines, and the remaining colonies were fixed with 4% paraformaldehyde at 4 weeks posttransfection and then stained with crystal violet. The number of colonies was counted (right). (D) Huh7OK1 cells transfected with 10 μ g of *in vitro*-transcribed full-length JFH-1 viral RNA were further transfected with siCntrl or siPA28 γ 1 at 24 hours posttransfection of viral RNA. The level of HCV core protein in the cells was determined by way of ELISA at 1 and 3 days posttransfection (left). Infectious virus titers in the culture supernatants at 1 and 3 days posttransfection were determined by way of focus-forming assay (middle). Infectious viral titers in the shCntrl or KD5 cells transfected with 10 μ g of the infectious viral RNA were determined at 5 days posttransfection (right). * $P < 0.05$, ** $P < 0.01$ versus the control cells or cells transfected with siCntrl. Data are representative of three independent experiments.



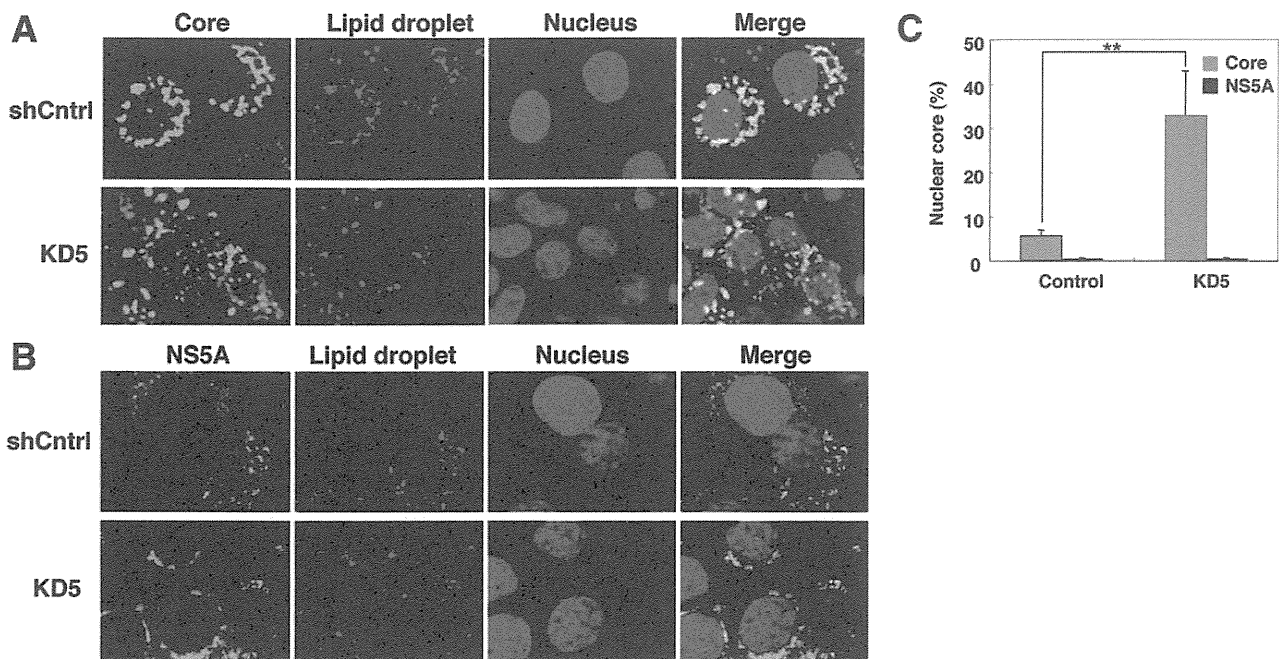


Fig. 4. Effect of PA28 γ knockdown on the localization of HCV core protein and lipid droplets. The shCntrl and KD5 cell lines infected with JFH-1 virus were fixed with methanol or paraformaldehyde for 5 minutes at 4 days postinfection. HCV core (A) and NS5A (B) proteins were stained with rabbit antibodies raised against the proteins and Alexa Fluor 488-conjugated goat anti-rabbit immunoglobulin G antibody. Lipid droplets were stained with Bodipy 558/568 C12. Nuclei were stained with 50 μ M Hechst 33258 after treatment with 1 μ g/mL of RNase A. Data are representative of three independent experiments. (C) The percentage of the area occupied by the core protein in nucleus and cytoplasm was calculated using the method described in Materials and Methods. The percentage of the nuclear NS5A to total NS5A was estimated by the same way as the ratio of the core protein. ** $P < 0.01$ versus control siRNA-transfected cells.

the PA28 γ knockdown condition. These results suggest that PA28 γ specifically regulates the postreplication steps in the life cycle of HCV.

Core Protein Is Partially Accumulated in the Nucleus of PA28 γ Knockdown Cells. We reported previously that some fraction of HCV core protein migrates into the nucleus and is then degraded by a PA28 γ -dependent proteasome pathway.⁷ Furthermore, we have demonstrated that HCV core protein is clearly accumulated in the nucleus of the liver cells of PA28 γ -knockout mice.⁸ However, the role of PA28 γ on the intracellular localization of HCV core protein in the infected HCV cells has not been characterized. HCV core protein was chiefly detected in cytoplasm of the control cell line infected with the JFH-1 virus, where it appeared around lipid droplets after staining with Bodipy 558/568 C12 (Fig. 4A, upper panels). In contrast, the core protein was detected not only in the cytoplasm around the surface of lipid droplets, but also in the nucleus in the KD5 cell line (Fig. 4A, lower panels). The NS5A protein was detected in the cytoplasm but not in the nucleus in both the shCntrl and KD5 cell lines (Fig. 4B). The percentage occupied by nuclear core protein to total core protein was increased by about six time levels in the KD5, while the ratio of nuclear NS5A to total NS5A exhibited no

difference (Fig. 4C). These results suggest that PA28 γ participates in the degradation of HCV core protein in the nucleus.

PA28 γ Positively Regulates HCV Propagation by Inhibiting Ubiquitin-Dependent Degradation of Core Protein in Cytoplasm. We reported previously that HCV core protein is degraded by at least two distinct pathways: a ubiquitin-dependent proteasome pathway and a ubiquitin-independent proteasome pathway.¹⁷ The ubiquitin E3 ligase, E6AP, can catalyze ubiquitin ligation of the core protein for ubiquitin-dependent degradation in the cytoplasm,¹⁸ whereas PA28 γ participates in the degradation of the core protein through a ubiquitin-independent pathway in the nucleus.¹⁷ We have also demonstrated that PA28 γ knockdown leads to enhanced ubiquitination of HCV core protein.⁸ However, the interplay between these two pathways in cells infected with HCV has not been determined. To address this point, we examined the effects of knockdown of E6AP or PA28 γ on the virus propagation and the ubiquitination of the core protein. JFH-1 virus was inoculated into E6AP- and/or PA28 γ knockdown cell lines (Fig. 5A). Transfection of the plasmid encoding shRNA to E6AP into the control cells (shCntrl) increased virus production (Fig. 5A [C-E]) in comparison with that of the

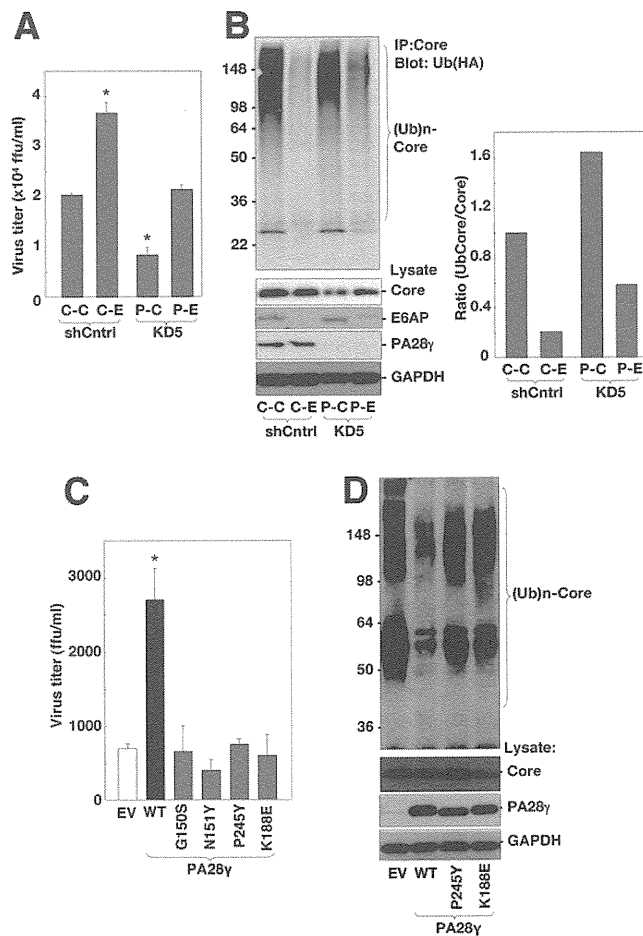


Fig. 5. PA28 γ knockdown enhances E6AP-dependent ubiquitination of core protein and reduces virus titer. (A) shCntrl and KD5 cells transfected with plasmids encoding the negative control (C-C and P-C) or E6AP (C-E and P-E) shRNA were treated with puromycin for 2 days. The remaining cells seeded at 2.5×10^4 cells in a 24-well plate were infected with the JFH-1 virus at an moi of 0.05, and infectious virus titers in the supernatants were determined at 72 hours postinfection by way of focus-forming assay. (B) The cells transfected and infected as in (A) were further transfected with a plasmid encoding HA-tagged ubiquitin at 48 hours postinfection. The cells were treated with 10 μ M MG132 for 5 hours at 72 hours postinfection and subjected to immunoprecipitation with anti-core monoclonal antibody and immunoblotting with anti-HA antibody. The ratio of ubiquitination of HCV core protein was assessed by the densitometries of the ubiquitinated and unubiquitinated core proteins. (C) KD5 cells transfected with plasmids encoding wild-type or mutant PA28 γ were infected with the JFH-1 virus at an moi of 0.05 at 24 hours posttransfection, and the infectious titers in the supernatant were determined at 72 hours postinfection by way of focus-forming assay. (D) KD5 cells transfected with plasmids encoding HCV core protein and HA-tagged ubiquitin, together with wild-type or mutant PA28 γ , were treated with 10 μ M MG132 for 5 hours at 24 hours posttransfection and subjected to immunoprecipitation with anti-core monoclonal antibody and immunoblotting with anti-HA antibody. EV, empty vector; WT, plasmid encoding wild-type PA28 γ . * $P < 0.05$ versus shCntrl or KD5 cells transfected with the negative control or empty vector. Data are representative of three independent experiments.

control cells transfected with the plasmid encoding control shRNA (Fig. 5A [C-C]). Furthermore, the impaired virus production in the PA28 γ knockdown

cells (KD5) was restored by the transfection of the plasmid encoding shRNA to E6AP (Fig. 5A [P-E]). Cells expressing hemagglutinin (HA)-tagged ubiquitin infected with the JFH-1 virus were immunoprecipitated by the anti-core antibody, and the immunoprecipitates were analyzed by immunoblotting with anti-HA antibody (Fig. 5B). E6AP knockdown decreased the ratio of ubiquitination of HCV core protein, in contrast to the increase of that by PA28 γ knockdown (Fig. 5B, lanes C-E and P-C). Furthermore, E6AP knockdown in the PA28 γ knockdown cells restored the ubiquitination of the core protein to a certain extent (Fig. 5B, lane P-E). It was shown that Pro²⁴⁵ of PA28 γ is critical for binding to the 20S proteasome, and that Gly¹⁵⁰ and Asn¹⁵¹ of PA28 γ are important for activation of the proteasome.²⁶ To further examine the functional significance of PA28 γ on HCV propagation, expression plasmids encoding siRNA-resistant PA28 γ mutants in which Gly¹⁵⁰, Asn¹⁵¹, and Pro²⁴⁵ were replaced with Ser (G150S), Tyr (N151Y), and Tyr (P245Y), respectively, were transfected into KD5 cells and inoculated with JFH-1 virus at 24 hours posttransfection. The infectious virus titers in the culture supernatant were determined at 3 days postinfection (Fig. 5C). KD5 cells transfected with the plasmid encoding wild-type PA28 γ exhibited a partial recovery of virus production, although those transfected with the plasmid encoding PA28 γ G150S, N151Y, or P245Y or with an empty vector exhibited no effect on virus production. Replacing Lys¹⁸⁸ with Glu in PA28 γ (PA28 γ K188E) confers the capability of proteasome-mediated cleavage after hydrophobic, acidic, and basic residues such as those exhibited by PA28 α .²⁷ Expression of siRNA-resistant PA28 γ K188E in KD5 cells could not restore virus production (Fig. 5D). The ubiquitination of HCV core protein was inhibited by expression of the wild-type PA28 γ but not expression of the PA28 γ mutants (P245Y or K188E) in KD5 cells (Fig. 5D). Collectively, these results suggest that PA28 γ positively regulates HCV propagation by inhibiting degradation of HCV core protein by an E6AP/ubiquitin-dependent proteasome.

Discussion

To explore the role of PA28 γ on the life cycle of HCV, we examined the effects of knockdown of PA28 γ in Huh7OK1 cells infected with the JFH-1 virus. Knockdown of PA28 γ in Huh7OK1 cells before or after infection with the JFH-1 virus impaired

production of infectious particles but did not impair viral RNA replication. However, PA28 γ knockdown did not affect the production of JEV, of which the capsid protein does not interact with PA28 γ , suggesting that PA28 γ knockdown does not affect the general sorting pathway of flavivirus. These results suggest that PA28 γ is specifically involved in the postreplication steps of HCV life cycle. Our previous report indicated that HCV core protein was accumulated in the nucleus of the hepatocytes of HCV core transgenic/PA28 γ knockout mice.⁸ PA28 γ is located mainly in the nucleus, although a small portion is also located in the cytoplasm^{7,28} and can up-regulate trypsin-like proteasome activity, which cleaves after basic amino acid residues.²⁷ Previous studies have shown that some fraction of HCV core protein is translocated into the nucleus and quickly degraded in the PA28 γ -dependent proteasome pathway.^{7,8,29} Miyanari et al.³⁰ demonstrated that the core protein is localized on the surface of lipid droplets and is surrounded by nonstructural proteins, suggesting that HCV particles are assembled near the surface of the lipid droplets. In the present experiments, although HCV core protein was detected on the surface of the lipid droplets in both control and PA28 γ knockdown cell lines, it was partially localized in the nucleus in PA28 γ knockdown cells but not control cells. Furthermore, localization of HCV core protein on the surface of lipid droplets was impaired in PA28 γ knockdown cells (Fig. 4). These results suggest that HCV core protein is partially translocated into the nucleus and degraded in the PA28 γ -dependent proteasome pathway in HCV-infected cells and that PA28 γ does not directly participate in the particle formation of HCV.

HCV core protein is degraded by at least two proteasome pathways: a ubiquitin-dependent pathway and a ubiquitin-independent and PA28 γ -dependent pathway.¹⁷ The E3 ligase E6AP catalyzes ubiquitin ligation to HCV core protein, resulting in enhanced degradation of the core protein in the cytoplasm.¹⁸ Knockdown of E6AP up-regulated virus production in cells infected with the JFH-1 virus,¹⁸ suggesting that E6AP/ubiquitin-dependent degradation of the core protein contributes to an antiviral response. In contrast, knockdown of PA28 γ induced up-regulation of the ubiquitination of HCV core protein and down-regulation of the viral production, suggesting that PA28 γ -dependent proteasome activity contributes to the proviral response by suppressing E6AP-dependent degradation of the core protein, thereby enhancing viral particle formation. The wild-type PA28 γ enhances the trypsin-like activity of proteasome that cleaves peptide bonds

after basic residues of the substrates, whereas the PA28 γ K188E mutant enhances the proteasome activity that cleaves peptide bonds after hydrophobic, acidic, and basic residues in the manner of PA28 α .²⁷ Therefore, the sizes of fragments produced by the PA28 γ -dependent proteasome should be different from those produced by the PA28 α/β - or ubiquitination-mediated proteasome. It might be feasible to speculate that the peptide fragments of HCV core protein generated by the PA28 γ -dependent proteasome or PA28 γ *per se* may be directly or indirectly involved in the suppression of the E6AP-dependent ubiquitination of the core protein. Further studies will be needed to clarify the relationship between E6AP and PA28 γ in the degradation and ubiquitination of HCV core protein. Figure 6 shows a schematic diagram of our hypothesis of the regulation of HCV propagation by PA28 γ .

HCV core protein was found in not only nuclei but also cytoplasm of the infected KD5 cells (Fig. 4). The down-regulation of virus production should potentially reduce a total amount of the core protein in KD5 cells before a clear accumulation of the core protein in nuclei. Furthermore, a small amount of PA28 γ was found in the PA28 γ knockdown cells, suggesting that E6AP-dependent degradation of HCV core protein is not potentially suppressed in the PA28 γ knockdown cells. If HCV core protein is constitutively expressed under the PA28 γ knockout cells regardless of an amount of infected virus, a clear accumulation of the core protein in nuclei should be found without cytoplasmic expression of the core protein under the PA28 γ knockout condition. We reported previously that HCC and liver steatosis in mouse are induced by the HCV core protein in the presence, but not the absence, of PA28 γ .⁸ Although HCV core protein is predominantly detected in the cytoplasm of the liver cells of PA28 $\gamma^{+/+}$ mice,^{8,31} HCV core protein was clearly accumulated in the nuclei, but clearly reduced in cytoplasm, of liver cells of PA28 $\gamma^{-/-}$ mouse.⁸ In addition, ubiquitination of HCV core protein was increased by PA28 γ knockdown in the 293T cell line.⁸ These results and the data in Fig. 5 suggest that the suppression of PA28 γ function enhances the E6AP-dependent degradation of HCV core protein. Hence, the reason there is no difference between PA28 $\gamma^{+/+}$ and PA28 $\gamma^{-/-}$ mice with respect to the amount of core protein may be due to the competitive regulation of the core protein by E6AP- and PA28 γ -dependent degradation mechanisms. E6AP-dependent degradation of HCV core protein in cytoplasm may be enhanced *in vivo* under the PA28 γ knockout condition.

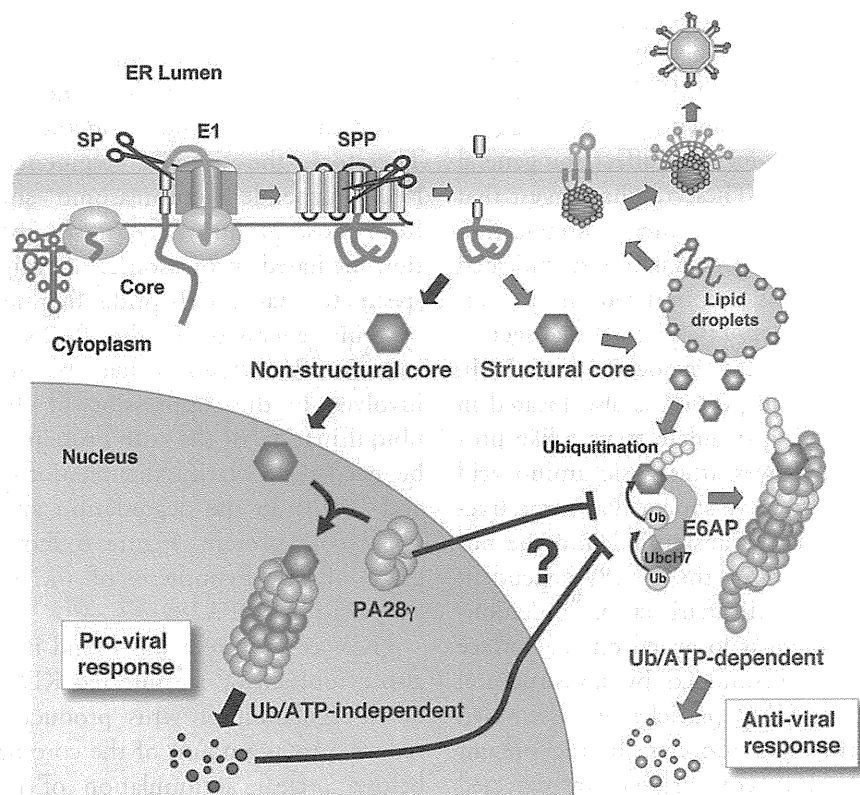


Fig. 6. Schematic diagram of the potential roles of PA28 γ in HCV propagation. HCV core protein is cleaved off from the precursor polyprotein by signal peptidase (SP) and the signal sequence is further processed by signal peptide peptidase (SPP). The mature core protein mainly localizes on the lipid droplets close to the endoplasmic reticulum to form a nucleocapsid with the viral RNA genome and is incorporated into virus particles as a structural protein. In addition to the structural protein of HCV, the core protein has characteristics of a nonstructural protein. HCV core protein is degraded through ubiquitin-dependent and ubiquitin-independent proteasome pathways. E6AP catalyzes ubiquitin ligation to HCV core protein and promotes degradation in the cytoplasm, which contributes to the antiviral response. In contrast, the core protein partially migrates into the nucleus and is degraded through a ubiquitin-independent and PA28 γ -dependent proteasome pathway, and the core protein fragments generated by the PA28 γ pathway or PA28 γ *per se* were suggested to participate in the suppression of E6AP-dependent ubiquitination of HCV core protein, which contributes to the proviral response.

In conclusion, in this study we demonstrated that the proteasome activator PA28 γ positively regulates particle production of HCV by inhibiting E6AP-dependent ubiquitination of the core protein, in addition to our previous observation that PA28 γ plays a crucial role in the development of liver pathology induced by HCV core protein.⁸ PA28 γ knockout mice exhibit only mild growth retardation.^{15,16} Therefore, PA28 γ may be a novel and promising antiviral target not only for elimination of HCV from hepatitis C patients but also for intervention in the progression of liver diseases induced by chronic HCV infection.

Acknowledgment: We thank H. Murase for her secretarial work. We also thank R. Bartenschlager and T. Wakita for providing cell lines and plasmids.

References

1. Wasley A, Alter MJ. Epidemiology of hepatitis C: geographic differences and temporal trends. *Semin Liver Dis* 2000;20:1-16.
2. Moriishi K, Matsuura Y. Host factors involved in the replication of hepatitis C virus. *Rev Med Virol* 2007;17:343-354.
3. Hussy P, Langen H, Mous J, Jacobsen H. Hepatitis C virus core protein: carboxy-terminal boundaries of two processed species suggest cleavage by a signal peptidase. *Virology* 1996;224:93-104.
4. Okamoto K, Mori Y, Komoda Y, Okamoto T, Okochi M, Takeda M, et al. Intramembrane processing by signal peptide peptidase regulates the membrane localization of hepatitis C virus core protein and viral propagation. *J Virol* 2008;82:8349-8361.
5. Barba G, Harper F, Harada T, Kohara M, Goulinet S, Matsuura Y, et al. Hepatitis C virus core protein shows a cytoplasmic localization and associates to cellular lipid storage droplets. *Proc Natl Acad Sci U S A* 1997;94:1200-1205.
6. Moriya K, Yotsuyanagi H, Shintani Y, Fujie H, Ishibashi K, Matsuura Y, et al. Hepatitis C virus core protein induces hepatic steatosis in transgenic mice. *J Gen Virol* 1997;78:1527-1531.
7. Moriishi K, Okabayashi T, Nakai K, Moriya K, Koike K, Murata S, et al. Proteasome activator PA28 γ -dependent nuclear retention and degradation of hepatitis C virus core protein. *J Virol* 2003;77:10237-10249.
8. Moriishi K, Mochizuki R, Moriya K, Miyamoto H, Mori Y, Abe T, et al. Critical role of PA28 γ in hepatitis C virus-associated steatogenesis and hepatocarcinogenesis. *Proc Natl Acad Sci U S A* 2007;104:1661-1666.
9. Miyamoto H, Moriishi K, Moriya K, Murata S, Tanaka K, Suzuki T, et al. Involvement of PA28 γ -dependent pathway in insulin resistance induced by hepatitis C virus core protein. *J Virol* 2007;81:1727-1735.

10. Li X, Lonard D, Jung SY, Malovannaya A, Feng Q, Qin J, et al. The SRC-3/AIB1 coactivator is degraded in a ubiquitin- and ATP-independent manner by the REGgamma proteasome. *Cell* 2006;124:381-392.
11. Zhang Z, Zhang R. Proteasome activator PA28 gamma regulates p53 by enhancing its MDM2-mediated degradation. *EMBO J* 2008;27:852-864.
12. Chen X, Barton LF, Chi Y, Clurman BE, Roberts JM. Ubiquitin-independent degradation of cell-cycle inhibitors by the REGgamma proteasome. *Mol Cell* 2007;26:843-852.
13. Li X, Amazit L, Long W, Lonard DM, Monaco JJ, O'Malley BW. Ubiquitin- and ATP-independent proteolytic turnover of p21 by the REGgamma-proteasome pathway. *Mol Cell* 2007;26:831-842.
14. Jariel-Encontre I, Bossis G, Piechaczyk M. Ubiquitin-independent degradation of proteins by the proteasome. *Biochim Biophys Acta* 2008;1786:153-177.
15. Barton LF, Runnels HA, Schell TD, Cho Y, Gibbons R, Tevethia SS, et al. Immune defects in 28-kDa proteasome activator gamma-deficient mice. *J Immunol* 2004;172:3948-3954.
16. Murata S, Kawahara H, Tohma S, Yamamoto K, Kasahara M, Nabe-shima Y, et al. Growth retardation in mice lacking the proteasome activator PA28gamma. *J Biol Chem* 1999;274:38211-38215.
17. Suzuki R, Moriishi K, Fukuda K, Shirakura M, Ishii K, Shoji I, et al. Proteasomal turnover of hepatitis C virus core protein is regulated by two distinct mechanisms: a ubiquitin-dependent mechanism and a ubiquitin-independent but PA28gamma-dependent mechanism. *J Virol* 2009;83:2389-2392.
18. Shirakura M, Murakami K, Ichimura T, Suzuki R, Shimoji T, Fukuda K, et al. E6AP ubiquitin ligase mediates ubiquitylation and degradation of hepatitis C virus core protein. *J Virol* 2007;81:1174-1185.
19. Aoyagi K, Ohue C, Iida K, Kimura T, Tanaka E, Kiyosawa K, et al. Development of a simple and highly sensitive enzyme immunoassay for hepatitis C virus core antigen. *J Clin Microbiol* 1999;37:1802-1808.
20. Lohmann V, Korner F, Koch J, Herian U, Theilmann L, Bartenschlager R. Replication of subgenomic hepatitis C virus RNAs in a hepatoma cell line. *Science* 1999;285:110-113.
21. Wakita T, Pietschmann T, Kato T, Date T, Miyamoto M, Zhao Z, et al. Production of infectious hepatitis C virus in tissue culture from a cloned viral genome. *Nat Med* 2005;11:791-796.
22. Pietschmann T, Lohmann V, Kaul A, Krieger N, Rinck G, Rutter G, et al. Persistent and transient replication of full-length hepatitis C virus genomes in cell culture. *J Virol* 2002;76:4008-4021.
23. Mori Y, Okabayashi T, Yamashita T, Zhao Z, Wakita T, Yasui K, et al. Nuclear localization of Japanese encephalitis virus core protein enhances viral replication. *J Virol* 2005;79:3448-3458.
24. Targett-Adams P, Chambers D, Gledhill S, Hope RG, Coy JF, Girod A, et al. Live cell analysis and targeting of the lipid droplet-binding adipocyte differentiation-related protein. *J Biol Chem* 2003;278:15998-16007.
25. Okamoto T, Omori H, Kaname Y, Abe T, Nishimura Y, Suzuki T, et al. A single-amino-acid mutation in hepatitis C virus NS5A disrupting FKBP8 interaction impairs viral replication. *J Virol* 2008;82:3480-3489.
26. Zhang Z, Clawson A, Realini C, Jensen CC, Knowlton JR, Hill CP, et al. Identification of an activation region in the proteasome activator REGalpha. *Proc Natl Acad Sci U S A* 1998;95:2807-2811.
27. Li J, Gao X, Ortega J, Nazif T, Joss L, Bogoy M, et al. Lysine 188 substitutions convert the pattern of proteasome activation by REGgamma to that of REGs alpha and beta. *EMBO J* 2001;20:3359-3369.
28. Nikaïdo T, Shimada K, Nishida Y, Lee RS, Pardee AB, Nishizuka Y. Loss in transformed cells of cell cycle regulation of expression of a nuclear protein recognized by SLE patient antisera. *Exp Cell Res* 1989;182:284-289.
29. Suzuki R, Sakamoto S, Tsutsumi T, Rikimaru A, Tanaka K, Shimoike T, et al. Molecular determinants for subcellular localization of hepatitis C virus core protein. *J Virol* 2005;79:1271-1281.
30. Miyanari Y, Atsuzawa K, Usuda N, Watashi K, Hishiki T, Zayas M, et al. The lipid droplet is an important organelle for hepatitis C virus production. *Nat Cell Biol* 2007;9:1089-1097.
31. Moriya K, Fujie H, Shintani Y, Yotsuyanagi H, Tsutsumi T, Ishibashi K, et al. The core protein of hepatitis C virus induces hepatocellular carcinoma in transgenic mice. *Nat Med* 1998;4:1065-1067.

Cochaperone Activity of Human Butyrate-Induced Transcript 1 Facilitates Hepatitis C Virus Replication through an Hsp90-Dependent Pathway[∇]

Shuhei Taguwa,¹ Hiroto Kambara,¹ Hiroko Omori,² Hideki Tani,¹ Takayuki Abe,¹ Yoshio Mori,¹ Tetsuro Suzuki,³ Tamotsu Yoshimori,² Kohji Moriishi,¹ and Yoshiharu Matsuura^{1*}

Department of Molecular Virology¹ and Department of Cellular Regulation,² Research Institute for Microbial Diseases, Osaka University, Osaka, and Department of Virology II, National Institute of Infectious Diseases, Tokyo,³ Japan

Received 21 May 2009/Accepted 27 July 2009

Hepatitis C virus (HCV) nonstructural protein 5A (NS5A) is a component of the replication complex consisting of several host and viral proteins. We have previously reported that human butyrate-induced transcript 1 (hB-ind1) recruits heat shock protein 90 (Hsp90) and FK506-binding protein 8 (FKBP8) to the replication complex through interaction with NS5A. To gain more insights into the biological functions of hB-ind1 in HCV replication, we assessed the potential cochaperone-like activity of hB-ind1, because it has significant homology with cochaperone p23, which regulates Hsp90 chaperone activity. The chimeric p23 in which the cochaperone domain was replaced with the p23-like domain of hB-ind1 exhibited cochaperone activity comparable to that of the authentic p23, inhibiting the glucocorticoid receptor signaling in an Hsp90-dependent manner. Conversely, the chimeric hB-ind1 in which the p23-like domain was replaced with the cochaperone domain of p23 resulted in the same level of recovery of HCV propagation as seen in the authentic hB-ind1 in cells with knockdown of the endogenous hB-ind1. Immunofluorescence analyses revealed that hB-ind1 was colocalized with NS5A, FKBP8, and double-stranded RNA in the HCV replicon cells. HCV replicon cells exhibited a more potent unfolded-protein response (UPR) than the parental and the cured cells upon treatment with an inhibitor for Hsp90. These results suggest that an Hsp90-dependent chaperone pathway incorporating hB-ind1 is involved in protein folding in the membranous web for the circumvention of the UPR and that it facilitates HCV replication.

Hepatitis C virus (HCV) is the major causative agent of non-A, non-B hepatitis in humans and infects approximately 170 million people worldwide (64). HCV belongs to the genus *Hepacivirus* of the family *Flaviviridae* and is classified into six major genotypes (39). The virus forms small, round, enveloped particles and possesses a genome consisting of a single positive-stranded RNA with a nucleotide length of 9.6 kb. The viral genome encodes a single precursor polyprotein consisting of approximately 3,000 amino acids, which in turn is posttranslationally processed into 10 viral proteins by host and viral proteases. The structural proteins are cleaved from the N-terminal one-fourth of the polyprotein by the host signal peptidase and signal peptide peptidase (36, 43, 44), resulting in the maturation of capsid protein, two envelope proteins, and viroporin p7. The nonstructural protein 2 (NS2) protease cleaves its own carboxyl terminus, and then NS3 cleaves the appropriate downstream positions to produce NS3, NS4A, NS4B, NS5A, and NS5B (24, 60), which form the replication complex, together with several host proteins (14, 35).

NS5A is a membrane-anchored zinc-binding phosphoprotein that appears to possess diverse functions, including the suppression of host defense and the regulation of virus replication (1, 15, 58), but its biological function remains unclear.

Several groups, including ours, have suggested that the molecular chaperone, heat shock protein 90 (Hsp90), and several cochaperones participate in the replication complex of HCV through interaction with NS5A or other NS proteins (45, 56, 65). Hsp90 is the highly conserved and ubiquitously expressed protein that acts as a key regulator for the turnover and the activities of more than 200 signaling proteins, including steroid receptors and cell-signaling kinases (66). The chaperone activity of Hsp90 contributes to the refolding of an unfolded protein in an ATP-dependent manner, and the execution of Hsp90-dependent protein folding requires the formation of a multi-chaperone complex containing other chaperones (e.g., Hsp70, Hsp104, and Hsp40) and cochaperones (e.g., p23, Hop, and immunophilins) (4, 18, 48). Geldanamycin or its derivatives, which are represented as specific inhibitors of Hsp90, can destabilize and then degrade client proteins (41, 55).

The host chaperone mechanism is involved in the folding of viral polymerase to support viral replication (6, 27). Moreover, host chaperones have been reported to play roles in the assembly of viral particles and the sorting of virus proteins (9, 32, 38). We have previously reported that Hsp90 chaperone activities and chaperone-associated proteins are required for the efficient propagation of HCV (45, 56) and that human butyrate-induced transcript 1 (hB-ind1) is involved in the propagation of HCV through interactions with NS5A and Hsp90 via the coiled-coil domain and the FXXW motif, respectively (56). hB-ind1 was first reported to be a multiple-membrane-spanning protein consisting of 362 amino acids that possesses a significant homology with a cochaperones, p23, that regulates

* Corresponding author. Mailing address: Department of Molecular Virology, Research Institute for Microbial Diseases, Osaka University, 3-1, Yamadaoka, Suita-shi, Osaka 565-0871, Japan. Phone: 81-6-6879-8340. Fax: 81-6-6879-8269. E-mail: matsuura@biken.osaka-u.ac.jp.

[∇] Published ahead of print on 5 August 2009.

Hsp90 function by its cochaperone activity (11). However, the roles of hB-ind1 in the life cycle of HCV have not been precisely clarified. In this study, we investigated the role of the Hsp90-related chaperone system, including hB-ind1, in the regulation of the RNA replication and particle production of HCV.

MATERIALS AND METHODS

Plasmids. The plasmids encoding hB-ind1, NS5A, Hsp90, and FK506-binding protein 8 (FKBP8) were prepared by methods described previously (45, 56). The DNA fragments encoding hB-ind1 mutants were prepared by PCR with the introduction of a silent mutation that is resistant to the short hairpin RNA in the hB-ind1 knockdown cells, as described previously (56). The human p23 gene and glucose-regulated protein 78 (GRP78) promoter region (−151 to +22) were amplified by PCR from the total cDNA and genomic DNA of Huh7 cells, respectively. The DNA fragments encoding mutants of hB-ind1 and p23 were prepared by the method of splicing by overlap extension (26) and introduced into pEF FLAGGs pGKpuro (28). The GRP78 promoter region was introduced between the KpnI and HindIII sites of pGL3-basic (Promega, Madison, WI) and designated pGRP78-luc. The reporter plasmid carrying a firefly luciferase gene under the control of the GR promoter (pGR-luc) was purchased from Panomics (Fremont, CA). The internal-control plasmid encoding a *Renilla* luciferase (pRL-TK) was purchased from Promega. The plasmid pFK-I₃₈₉ neo/NS3-3'/NK5.1 (47) was kindly provided by R. Bartenschlager. The plasmids used in this study were confirmed by sequencing them with an ABI Prism 3130 genetic analyzer (Applied Biosystems, Tokyo, Japan).

Cells and virus infection. All cell lines were cultured at 37°C under a humidified atmosphere and 5% CO₂. The human embryonic kidney 293T and hepatocellular carcinoma Huh7 cell lines were maintained in Dulbecco's modified Eagle's medium (DMEM) (Sigma, St. Louis, MO) supplemented with 100 U/ml penicillin, 100 µg/ml streptomycin, and 10% fetal calf serum (FCS). The human hepatocellular carcinoma cell line Huh7.5.1 was kindly provided by F. Chisari (70) and was maintained in DMEM containing nonessential amino acids, 100 U/ml penicillin, 100 µg/ml streptomycin, and 10% FCS. The Huh9-13 cell line, which is a Huh7 cell line harboring a subgenomic HCV RNA replicon (35), was maintained in DMEM containing 10% FCS, nonessential amino acids, and 1 mg/ml G418 (Nakalai Tesque, Kyoto, Japan). The hB-ind1 knockdown cell line Huh-KD and control cell line Huh-ctrl were described previously (56). Huh-KD cells were transfected with each of the expression plasmids encoding wild-type or mutant hB-ind1 and cultured for 1 week in the presence of 10 µg/ml of puromycin. The remaining cells were used for the experiments described below. The viral RNA of JFH1 was introduced into Huh7.5.1 cells according to the method of Wakita et al. (62) for preparation of the infectious HCV particles in cell culture.

Antibodies. The rabbit anti-hB-ind1 antibody was prepared as described previously (56). Mouse monoclonal antibodies to HCV NS5A, influenza virus hemagglutinin (HA) and FLAG tags, and β-actin were purchased from Austral Biologicals (San Ramon, CA), Covance (Richmond, CA), and Sigma, respectively. Mouse anti-protein disulfide isomerase (PDI) immunoglobulin G2a (IgG2a) was from Affinity Bioreagents (Golden, CO). Mouse anti-double-stranded RNA (dsRNA) IgG2a (J1 and K2) antibodies were from Biocenter Ltd. (Szirak, Hungary). Alexa Fluor 488 (AF488)-conjugated anti-mouse IgG1, AF647-conjugated anti-rabbit IgG, and AF594-conjugated anti-mouse IgG2a and IgG2b antibodies were from Invitrogen (San Diego, CA).

Transfection, immunoblotting, and immunoprecipitation. Transfection and immunoprecipitation analyses were carried out as described previously (25, 45). Immunoprecipitates boiled in loading buffer were subjected to 12.5% sodium dodecyl sulfate-polyacrylamide gel electrophoresis. The proteins were transferred to polyvinylidene difluoride membranes (Millipore, Bedford, MA) and were reacted with the appropriate antibodies. The immune complexes were visualized with Super Signal West Femto substrate (Pierce, Rockford, IL) and detected by an LAS-3000 image analyzer system (Fujifilm, Tokyo, Japan). The protein bands of GRP78 and β-actin were quantified by Multi Gauge software (Fujifilm), and the values of GRP78 expression were normalized with those of β-actin.

Quantitative reverse transcriptase PCR. HCV RNA was estimated by the method described previously (56). Total RNA was prepared from cells by using an RNeasy minikit (Qiagen, Tokyo, Japan). First-strand cDNA was synthesized using an RNA LA PCR in vitro cloning kit (Takara Bio Inc., Shiga, Japan) and random primers. Each cDNA was estimated with Platinum SYBR green qPCR SuperMix UDG (Invitrogen) according to the manufacturer's protocol. Fluorescent signals were analyzed with an ABI Prism 7000 (Applied Biosystems). The

internal ribosomal entry site regions of HCV and mRNAs of GAPDH (glyceraldehyde-3-phosphate dehydrogenase), GRP78, and growth arrest- and DNA damage-inducible gene 153 (GADD153) were amplified using the primer pairs 5'-GAGTGTCTGTCAGCCTCCA-3' and 5'-CACTCGCAAGCACCTATC A-3', 5'-GAAGGTGAAGGTCGGAGTC-3' and 5'-GAAGGTGAAGGTCGG AGTC-3', 5'-CGCCAAGCGGCTCATC-3' and 5'-AACCACCTTGAACGGC AAGA-3', and 5'-AGCTGGAACCTGAGGAGAGA-3' and 5'-TGGATCAGT CTGGA AAAAGCA-3', respectively. The values of the HCV genome or each mRNA were normalized with those of GAPDH mRNA. Each PCR product was detected as a single band of the correct size on agarose gel electrophoresis (data not shown).

In vitro transcription and RNA transfection. The plasmid pFK-I₃₈₉ neo/NS3-3'/NK5.1 was linearized by treatment with Scal and then transcribed in vitro using the MEGascript T7 kit (Applied Biosystems) according to the manufacturer's protocol. The in vitro-transcribed RNA was electroporated into cells at 4 million cells/0.4 ml under conditions of 270 V and 960 µF using a Gene Pulser (Bio-Rad, Hercules, CA). The colony formation assay was carried out by a method described previously (45).

Indirect immunofluorescence assay. Cells cultured on glass slides were fixed with 4% paraformaldehyde in phosphate-buffered saline (PBS) at room temperature for 30 min. After being washed twice with PBS, the cells were permeabilized for 20 min at room temperature with PBS containing 0.25% saponin and blocked with PBS containing 0.2% gelatin (gelatin-PBS) for 60 min at room temperature. The cells were incubated with gelatin-PBS containing rabbit anti-hB-ind1 antibody, mouse anti-NS5A IgG1, mouse anti-PDI IgG2a, mouse anti-FKBP8 IgG2b, or mouse anti-dsRNA IgG2a (J1 and K2) at 37°C for 60 min; washed three times with PBS containing 1% Tween 20; and incubated with gelatin-PBS containing AF488-conjugated anti-mouse IgG1 or AF647-conjugated anti-rabbit or AF594-conjugated anti-mouse IgG2a or IgG2b antibodies at 37°C for 60 min. Finally, the cells were washed three times with PBS containing 1% Tween 20 and observed with a FluoView FV1000 laser scanning confocal microscope (Olympus, Tokyo, Japan).

Correlative FM-EM. Correlative fluorescence microscopy-electron microscopy (FM-EM) allows individual cells to be examined both in an overview with FM and in a detailed subcellular-structure view with EM (51). The endogenous hB-ind1 and NS5A were stained and observed in the HCV replicon cells by the correlative FM-EM method as described previously (45).

Luciferase assay. Each plasmid was transfected into Huh7, Huh9-13, and interferon (IFN)-cured cells seeded in a 12-well plate, and the cells were treated with 1 µM dexamethasone (Sigma) for 12 h or with 17-dimethylamino-ethylamino-17-demethoxygeldanamycin (DMAG) (Sigma) for 6 h at 36 h posttransfection and lysed in 200 µl of passive lysis buffer (Promega). Luciferase activity was measured in 20-µl aliquots of the cell lysates using a Dual-Luciferase Reporter Assay System (Promega). Firefly luciferase activity was standardized with that of *Renilla* luciferase cotransfected with the internal-control plasmid pRL-TK. The resulting values were expressed as the increase in relative light units (RLU).

Statistical analysis. Results were expressed as the mean ± standard deviation. The significance of differences in the means was determined by Student's *t* test.

RESULTS

The p23-like domain of hB-ind1 has cochaperone activity. Although we had previously reported that hB-ind1 regulates HCV RNA replication through interaction with NS5A and Hsp90, the molecular mechanisms underlying the regulation of HCV replication remained to be clarified. To gain more insights into the potential cochaperone activity of hB-ind1 in the Hsp90 chaperone system, we prepared expression plasmids encoding a wild-type p23 and three p23 mutants—one in which the FXXW motif was replaced with AXXA (p23AxxA), one in which the cochaperone domain of p23 was replaced with the p23-like domain of hB-ind1 (cp23), and one in which both substitutions were made (cp23AxxA) (Fig. 1A). HA-tagged Hsp90 was coexpressed with FLAG-tagged p23 or the FLAG-tagged p23 mutants in 293T cells (Fig. 1B). Hsp90 was coimmunoprecipitated with wild-type p23 and a cp23 mutant, but not with the p23AxxA or cp23AxxA mutants, indicating that the FXXW motif of hB-ind1, as is the case with that of p23

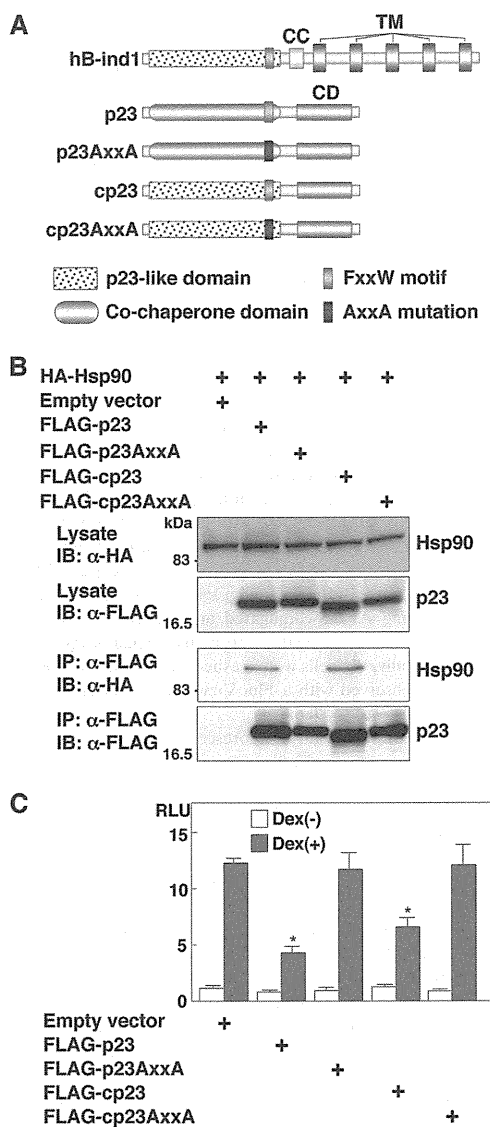


FIG. 1. Construction and characterization of p23 mutants. (A) Structures of hB-ind1, p23, and the three p23 mutants. hB-ind1 consists of a p23-like domain, an FXXW motif, a coiled-coil domain (CC), and a transmembrane domain (TM). p23 consists of a co-chaperone domain, an FXXW motif, and a chaperone domain (CD). The three p23 mutants, p23AxxA, cp23, and cp23AxxA, were constructed by replacing the FXXW motif with AXXA, the co-chaperone domain of p23 with the p23-like domain of hB-ind1, and both of the regions, respectively. (B) FLAG-tagged p23, p23AxxA, cp23, or cp23AxxA was coexpressed with HA-tagged Hsp90 in 293T cells and immunoprecipitated (IP) with anti-FLAG antibody. The immunoprecipitates were subjected to immunoblotting (IB). (C) The expression plasmid encoding FLAG-tagged p23, cp23, p23AxxA, or cp23AxxA was cotransfected with pGR-luc and pRL-TK plasmids into 293T cells and treated with 1 mM dexamethasone [Dex(+)] at 36 h posttransfection or untreated [Dex(-)], and the luciferase activities were determined at 12 h of incubation. The firefly luciferase activity was normalized with that of *Renilla* luciferase, and the GR-responsive promoter activity was indicated as the RLU. The error bars indicate standard deviations. The asterisks indicate significant differences ($P < 0.01$) versus the control value. The data shown are representative of three independent experiments.

(67), is also involved in binding to Hsp90. Hsp90 participates in the folding and stabilization of the ligand-binding domain of the glucocorticoid receptor (GR), together with p23 and other cofactors (49). p23 was shown to act not only in the activation (30), but also in the inhibition, of GR signaling (67). To examine whether hB-ind1 has the ability to work as a cochaperone in an Hsp90-dependent manner, each of the plasmids encoding p23 or the p23 mutants was cotransfected with a reporter plasmid carrying a firefly luciferase gene under the control of the GR promoter (pGR-luc), together with an internal-control plasmid (pRL-TK), and GR-mediated transcriptional activity was determined at 12 h after treatment with dexamethasone, a ligand of GR. Expression of the p23 or cp23 mutant, but not of the AXXA mutants, significantly inhibited GR-mediated transcription (Fig. 1C). These results indicate that the p23-like domain of hB-ind1 possesses cochaperone activity comparable to that of p23.

The p23-like domain of hB-ind1 is interchangeable with the p23 cochaperone domain during complex formation with NS5A, Hsp90, and FKBP8. Previous reports have suggested that HCV NS5A interacts with several host proteins, including FBL2 (63), vesicle-associated membrane protein-associated protein subtype A (VAP-A) (61), VAP-B (25), FKBP8 (45), and hB-ind1 (56), and that these interactions participate in the replication of HCV. We have shown that hB-ind1 interacts with NS5A and Hsp90 through the coiled-coil domain and the FXXW motif in the p23-like domain, respectively, and that coexpression of FKBP8 enhances the interaction of Hsp90 with hB-ind1 (56). To determine the effect of the mutation in the p23-like domain of hB-ind1 on interaction with Hsp90, NS5A, and FKBP8, we prepared an expression plasmid encoding wild-type hB-ind1 and three hB-ind1 mutants, one in which the p23-like domain was replaced with the cochaperone domain of p23 (chB-ind1), one in which the FXXW motif was replaced with AXXA (hB-ind1AxxA), and one in which both replacements were made (chB-ind1AxxA) (Fig. 2A). The FLAG-tagged wild-type or mutant hB-ind1 was coexpressed with HA-tagged Hsp90 (Fig. 2B, left) or HA-tagged NS5A (Fig. 2B, right) in 293T cells and immunoprecipitated with anti-FLAG antibody. Hsp90 was coprecipitated with wild-type hB-ind1 and the chB-ind1 mutant, but not with the hB-ind1AxxA and chB-ind1AxxA mutants (Fig. 2B, left), confirming that the FXXW motif is crucial for the interaction with Hsp90. In contrast, NS5A was coprecipitated with each of the hB-ind1 proteins, suggesting that mutation in the p23-like domain of hB-ind1 has no effect on the binding of hB-ind1 to NS5A through the coiled-coil domain (Fig. 2B, right). To determine the effect of FKBP8 expression on the interaction between hB-ind1 and Hsp90, FLAG-tagged wild-type hB-ind1 or the chB-ind1 mutant was coexpressed with HA-tagged FKBP8 and/or Hsp90 in 293T cells and immunoprecipitated with anti-FLAG antibody. The amounts of Hsp90 coprecipitated with hB-ind1 or chB-ind1 were increased by coexpression of FKBP8 (Fig. 2C). To further examine the interaction of hB-ind1 with Hsp90 and NS5A at an endogenous expression level in Huh9-13 cells harboring an HCV subgenomic RNA replicon, lysates of the replicon cells were subjected to immunoprecipitation analysis. Endogenous Hsp90 and NS5A were specifically coimmunoprecipitated with endogenous hB-ind1 (Fig. 2D). These results suggest that the p23-like domain of hB-ind1 is inter-

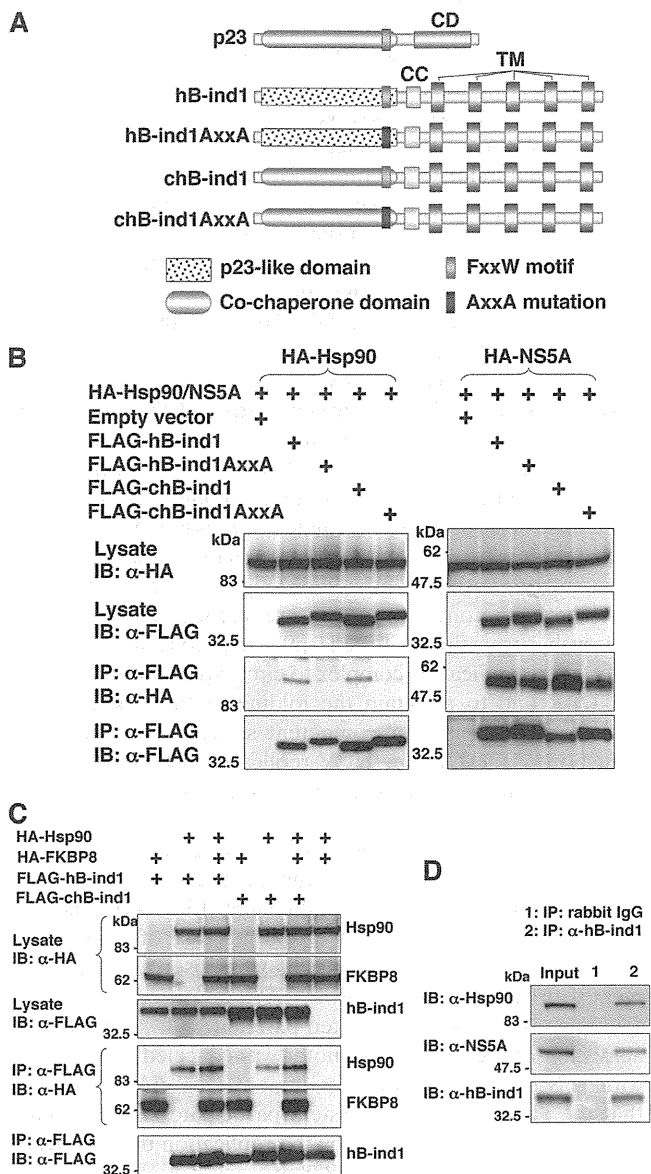


FIG. 2. Construction and characterization of hB-ind1 mutants. (A) Structures of p23, hB-ind1, and the three hB-ind1 mutants. The three hB-ind1 mutants, hB-ind1AxxA, chB-ind1, and chB-ind1AxxA, were constructed by replacing the FXXW motif with AXXA, the p23-like domain of hB-ind1 with the co-chaperone domain of p23, and both of the regions, respectively. (B) FLAG-tagged hB-ind1, hB-ind1AxxA, chB-ind1, or chB-ind1AxxA was coexpressed with either HA-tagged Hsp90 (left) or NS5A (right) in 293T cells and immunoprecipitated (IP) with anti-FLAG antibody. The immunoprecipitates were subjected to immunoblotting (IB). (C) HA-tagged Hsp90 and HA-FKBP8 were expressed with FLAG-tagged hB-ind1 and chB-ind1 in various combinations in 293T cells and immunoprecipitated with anti-FLAG antibody, and the immunoprecipitates were detected by immunoblotting. (D) Endogenous hB-ind1 in Huh9-13 cells harboring subgenomic HCV replicon RNA was immunoprecipitated with anti-hB-ind1 rabbit IgG (lane 2). The cell lysate was mixed with normal rabbit IgG as a negative control (lane 1). The immunoprecipitates were analyzed by immunoblotting with an antibody to Hsp90, NS5A, or hB-ind1. The data shown are representative of three independent experiments.

changeable with the co-chaperone domain of p23 during complex formation with NS5A, Hsp90, and FKBP8.

Cochaperone activity in the p23-like domain of hB-ind1 is required for propagation of HCV. The p23-like domain of hB-ind1 has been suggested to be required for HCV propagation (56). However, the involvement of the co-chaperone activity of hB-ind1 in HCV propagation has not been examined. To assess the effect of co-chaperone activity in the p23-like domain of hB-ind1 on the RNA replication and particle production of HCV, each of the expression plasmids encoding the FLAG-tagged wild-type or mutant hB-ind1 carrying the silent mutations resistant to small interfering RNA was transfected into hB-ind1 knockdown (Huh-KD) cells and cultured for a week in the presence of puromycin. The expressions of FLAG-tagged hB-ind1 and the mutants in the Huh-KD cells were comparable to that of the endogenous hB-ind1 in the control (Huh-ctrl) cells transfected with an empty vector (Fig. 3A). Subgenomic HCV replicon RNA transcribed from pFK-I₃₈₉ neo/NS3-3'/NK5.1 was transfected into these cells and cultured for 4 weeks in the presence of G418. Although the number of colonies was reduced in the Huh-KD cells compared with the Huh-ctrl cells after transfection with an empty vector, as described previously (56), the colony numbers were recovered by the expression of the hB-ind1 or chB-ind1 mutant, but not by that of the hB-ind1AxxA or chB-ind1AxxA mutants (Fig. 3B). Similarly, intracellular HCV RNA and infectious viral titers in the culture supernatants of Huh-KD cells infected with JFH1 virus were partially recovered by the expression of the hB-ind1 or chB-ind1 mutant, but not by that of the hB-ind1AxxA or chB-ind1AxxA mutant (Fig. 3C). These results suggest that co-chaperone activity in the p23-like domain of hB-ind1 is required for HCV propagation and that the co-chaperone domain of p23 can substitute for the p23-like domain of hB-ind1.

hB-ind1 colocalizes with NS5A, FKBP8, and dsRNA on the membranous web. Our previous report revealed the interplay among hB-ind1, Hsp90, FKBP8, and NS5A and showed that these interactions play an important role in HCV replication (56). However, the subcellular localization of the endogenous hB-ind1 in the replicon cells and JFH1 virus-infected cells has not been precisely assessed. To determine the subcellular localization of hB-ind1 in the context of HCV replication, the expression of hB-ind1 and NS5A in the replicon cells and JFH1 virus-infected cells was examined by immunofluorescence analyses (Fig. 4A). Endogenous hB-ind1 was colocalized with the endoplasmic reticulum (ER)-marker PDI and NS5A as dot-like structures in the Huh9-13 replicon cells (Fig. 4A, top) and in cells infected with JFH1 virus (Fig. 4A, bottom), and these dot-like structures disappeared in concert with the loss of NS5A expression by treatment with IFN- α in the replicon cells and was not observed in the mock-infected Huh7.5.1 cells. Furthermore, FKBP8 (Fig. 4B, top) and dsRNA (Fig. 4B, bottom) were colocalized with hB-ind1 and NS5A in the dot-like structures in Huh9-13 replicon cells. These results indicate that HCV replicating RNA is localized with hB-ind1, FKBP8, and NS5A in the dot-like compartments. HCV RNA replication or expression of viral proteins leads to formation of the convoluted membranous structures designated the membranous web (14, 23). The large structures of the replication complexes in the replicon cells indicate membranous webs with

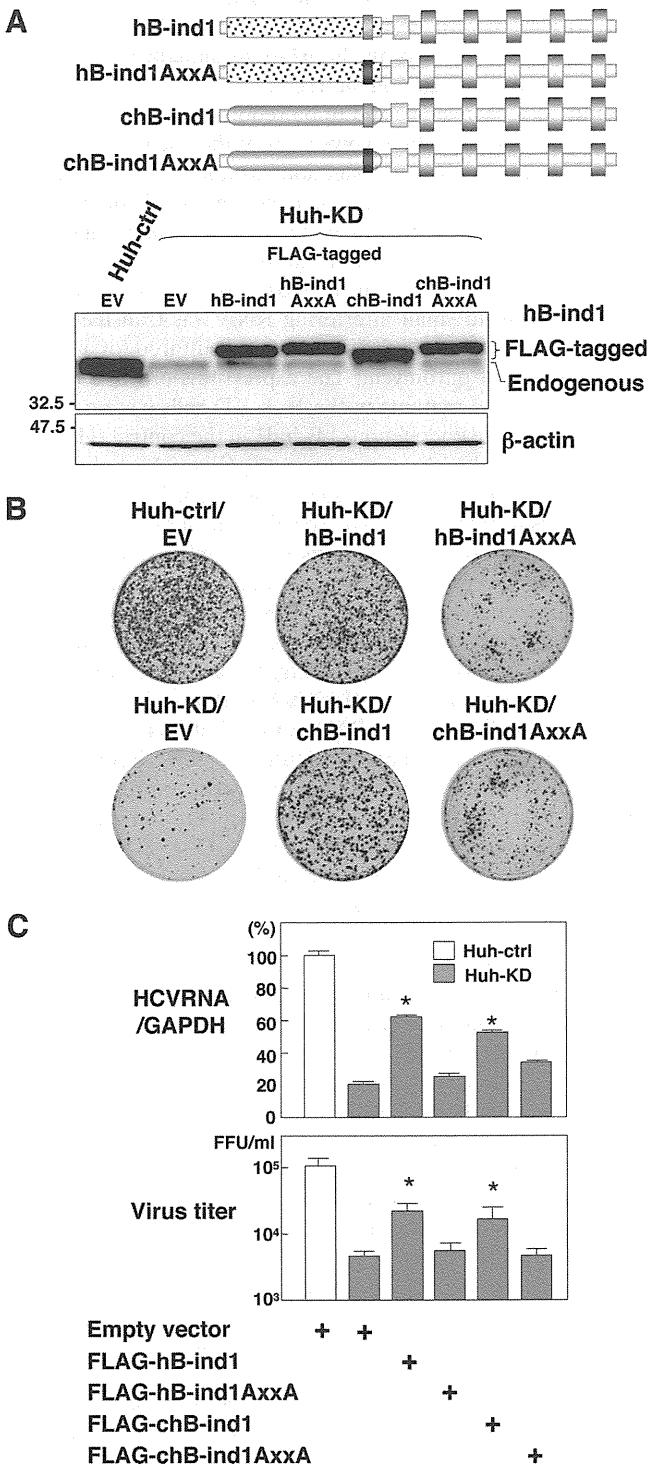


FIG. 3. Effects of the cochaperone activity of hB-ind1 on the propagation of HCV. (A) Huh-KD cells were transfected with either an empty vector or an expression plasmid encoding FLAG-tagged hB-ind1, hB-ind1AxxA, chB-ind1, or chB-ind1AxxA, which are resistant to small interfering RNA due to the introduction of silent mutations, and cultured for a week in the presence of 10 μg/ml of puromycin. The surviving cells were used in the subsequent experiments. The endogenous and exogenous expression of hB-ind1 and the mutants was detected by immunoblotting. The control cell line (Huh-ctrl) or the Huh-KD cell line transfected with an empty vector (EV) was used as a control. (B) Huh-KD cells were transfected with the plasmids and

restricted motility (68). To further analyze the subcellular compartments, including hB-ind1 and NS5A, the same field of the Huh9-13 replicon cells was observed under FM and EM by using the correlative FM-EM technique (Fig. 5A, upper two rows). The large structures that included hB-ind1 and NS5A in the replicon cells were observed under FM and EM (white-boxed areas) and further magnified (black-boxed areas). Convoluted membranous structures that consisted of small vesicles and that were similar to the membranous web were observed. Another field of view yielded similar results (Fig. 5A, lower two rows). The membranous web resembling the convoluted structures was not observed in the Huh9-13 cells depleted of viral RNA by IFN treatment (Fig. 5B). Together, these results suggest that hB-ind1 interacts with NS5A on the membranous web in cells replicating HCV RNA.

Hsp90 is involved in the circumvention of the UPR during HCV replication. Hsp90 regulates the folding and stability of proteins in all eukaryotes (59), and inhibition of the chaperone pathway suppresses correct protein folding, which leads to induction of proteasome-mediated degradation of the unfolded proteins and the unfolded protein response (UPR). Our previous (46) and present studies (Fig. 4 and 5) showed that several cochaperone components are recruited in the membranous web, suggesting that the Hsp90 chaperone system participates in the replication complex to circumvent the induction of the UPR and to maintain the folding of the host and viral proteins in a replication-competent state. To determine the induction of the UPR by HCV replication, Huh9-13 replicon cells were transfected with a reporter plasmid carrying a firefly luciferase gene under the control of the GRP78 promoter, which is activated by the induction of the UPR, together with an internal-control plasmid. Although the GRP78 promoter activity was slightly enhanced in the Huh9-13 cells compared to that in the parental cells, a fourfold increase of GRP78 promoter activity in the replicon cells was observed after treatment with an Hsp90 inhibitor, DMAG, in contrast to the two-fold increase in similarly treated parental Huh7 cells, and the activation of the GRP78 promoter was canceled by treatment with IFN-α despite DMAG treatment (Fig. 6A), suggesting that the Hsp90 chaperone system participates in the circumvention of the UPR induced by the replication of HCV RNA. In addition, activation of GRP78 at transcriptional and translational levels after treatment with DMAG was higher in the

then selected with puromycin. The resulting cells were further transfected with a replicon RNA transcribed from pFK-I₃₈₉ neo/NS3-3'/NK5.1, cultured for 4 weeks in the presence of 1 mg/ml of G418, and stained with crystal violet after fixation with 4% paraformaldehyde. The Huh-KD cell line transfected with an empty vector (EV) was used as a positive control. (C) The cells prepared as described above were infected with JFH1 virus and harvested at 3 days postinfection. The amount of intracellular HCV RNA was estimated by quantitative reverse transcriptase PCR and normalized with that of GAPDH mRNA. The values of HCV RNA are presented as percentages versus those of Huh-ctrl cells transfected with an empty vector. The culture supernatants were subjected to a focus-forming assay. Virus titers are presented as focus-forming units (FFU) per ml. The error bars indicate standard deviations. The asterisks indicate significant differences ($P < 0.01$) versus the value of the control. The data shown are representative of three independent experiments.

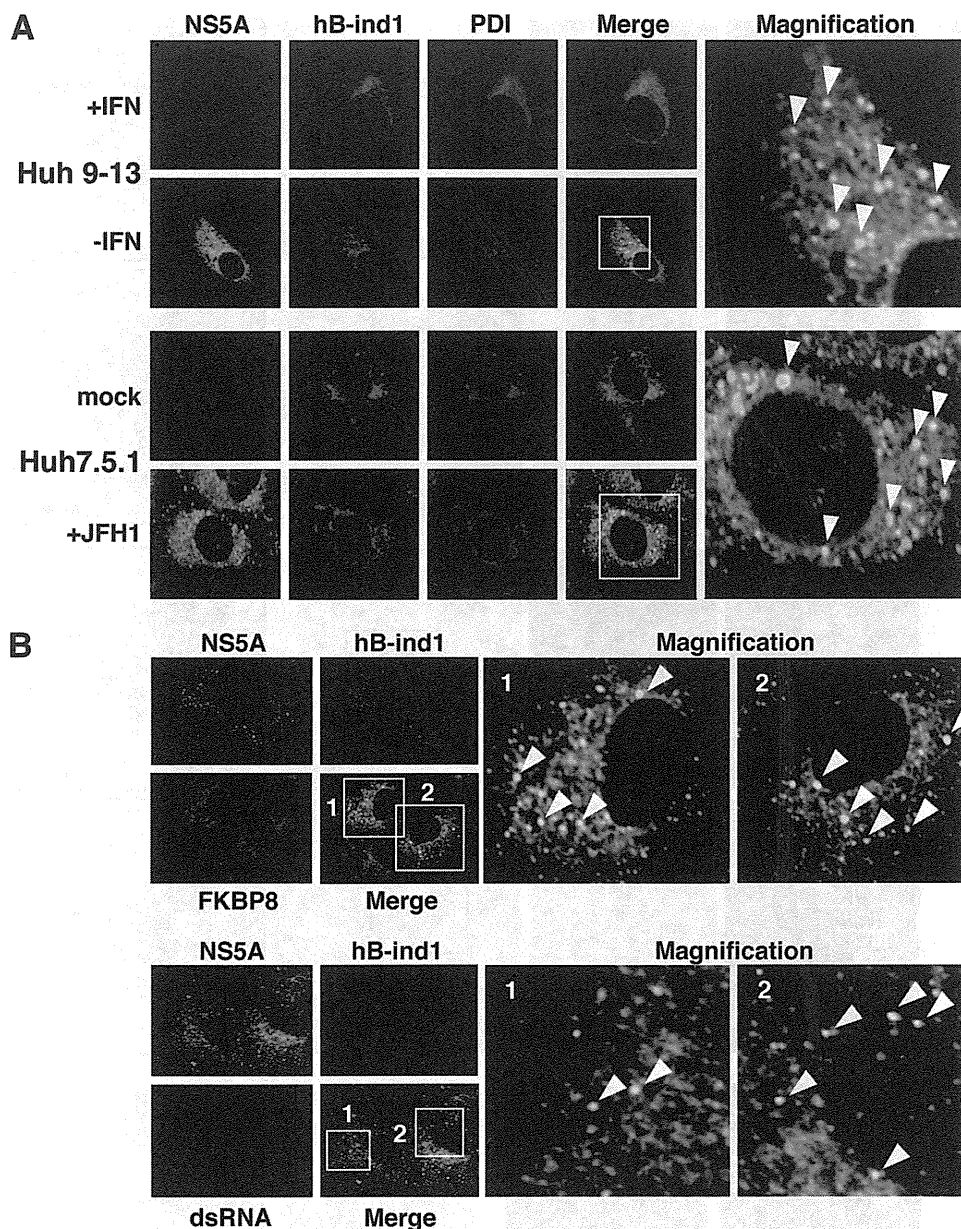


FIG. 4. Intracellular localization of hB-ind1 in replicon cells and infected cells. (A) Huh9-13 replicon cells with IFN- α or untreated and Huh7.5.1 cells infected with JFH1 virus or naïve cells were stained with antibodies against NS5A, hB-ind1, or PDI and examined by immunofluorescence assay. The boxed areas in the merged images are magnified and displayed on the right. The arrowheads indicate intracellular positions colocalized with NS5A, hB-ind1, and PDI. (B) Huh9-13 replicon cells were fixed, permeabilized, and stained with appropriate antibodies to NS5A, hB-ind1, and FKBP8 (top) or dsRNA (bottom). The boxed areas in the merged images are magnified and displayed on the right. The arrowheads indicate intracellular positions colocalized with NS5A, hB-ind, and FKBP8 or dsRNA. The images shown are representative of three independent experiments.

HCV replicon cells than in the parental cells or in cured cells, which were depleted of HCV RNA by treatment with IFN- α (Fig. 6B). Furthermore, DMAG treatment enhanced the transcription of the UPR marker protein GADD153 at a higher level in the replicon cells than in the parental Huh7 or the cured cells (Fig. 6C). These results suggest that the Hsp90-dependent chaperone system plays a crucial role in the folding of the host and viral proteins involved in HCV replication and in the regulation of UPR induction.

DISCUSSION

Studies of the relationship between Hsp90 and steroid receptors, such as GR, have revealed the activities of cochaperones (52, 67). Cochaperones, such as p23, appear to interact with and dissociate from Hsp90 and the client protein complex in a defined order. These cochaperones participate in the chaperone complex in a late step and promote the dissociation of the client proteins from Hsp90 to facilitate formation of the

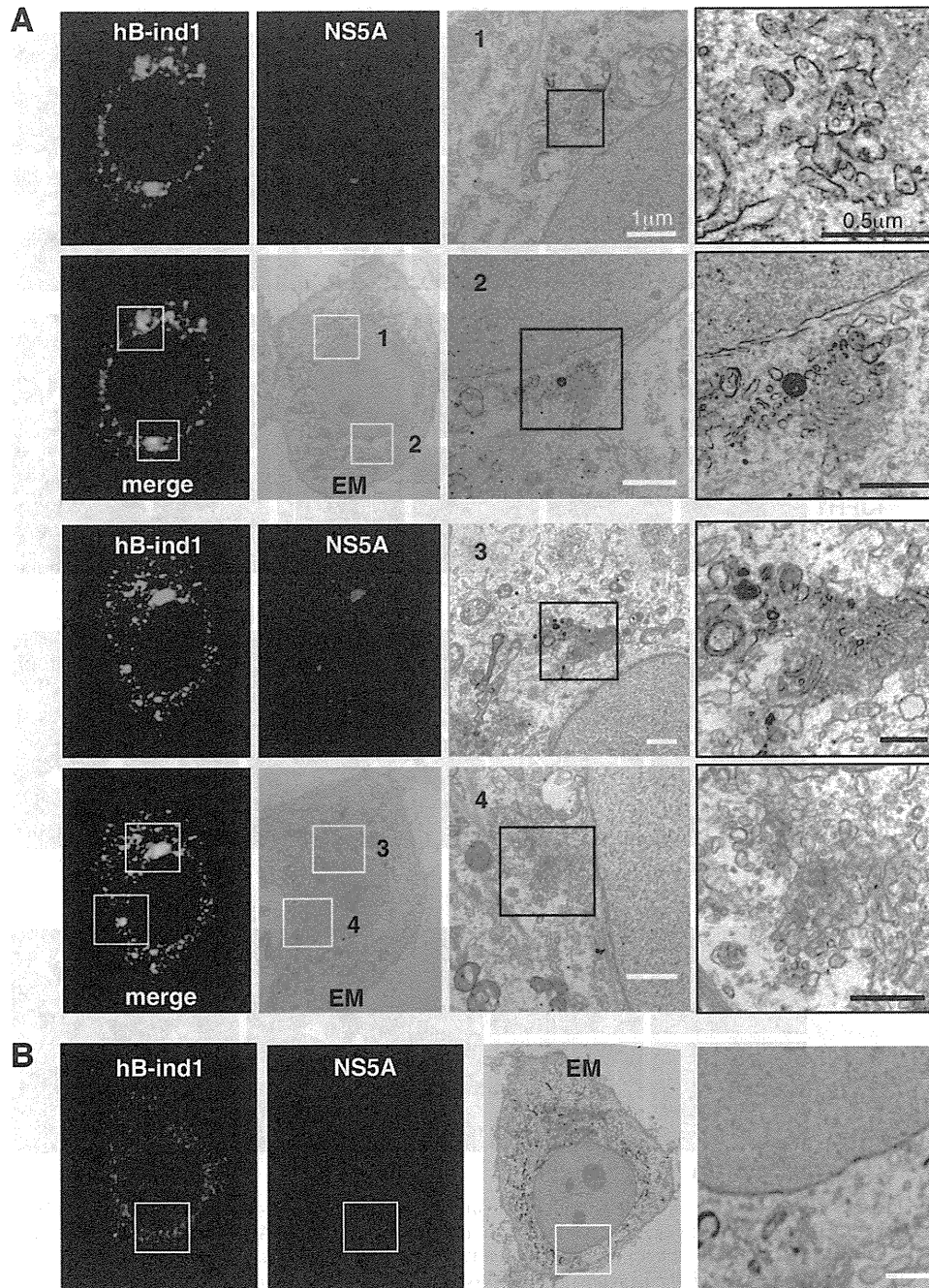


FIG. 5. hB-ind1 interacts with NS5A in the membranous web. Huh9-13 replicon cells were stained with specific antibodies to hB-ind1 and NS5A. Identical fields of Huh9-13 (A) or the cured cells (B) were observed under EM by using the correlative FM-EM technique. The white-boxed areas indicate the colocalized areas of hB-ind1 with NS5A. Magnified views of the white-boxed areas are displayed in the third column from the left. The right column contains further-magnified images of each of the black-boxed areas. Another field of view is presented in the lower two rows.

chaperone complex in the next chaperone cycle (16–18). In this study, we have shown that hB-ind1 participates in HCV replication and that the p23-like domain of hB-ind1 possesses co-chaperone activity comparable to that of the cochaperone domain of p23, suggesting that hB-ind1 is involved in the recycling of the chaperone complex in the membranous web to maintain the function of the replication complex of HCV.

Previous studies have indicated that HCV proteins rear-

range the ER membrane into the small convoluted membranous vesicles that are collectively known as the membranous web, and these vesicles have been suggested to be the intracellular compartments in which HCV replication takes place (14, 23, 68). In the living replicon cells, two forms of replication complexes, small and large vesicles, are detected, both of which include the viral replication complexes (68). Large vesicles, corresponding to membranous webs, exhibit restricted motil-

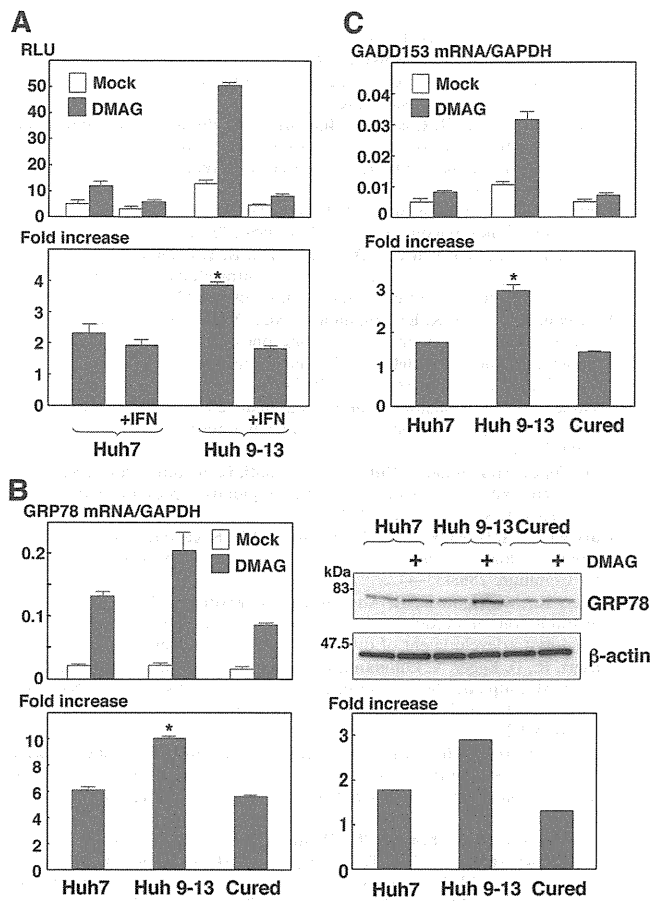


FIG. 6. Effect of Hsp90 inhibitor on the induction of the UPR in HCV replicon cells. (A) Huh7 and Huh9-13 replicon cells were transfected with a reporter plasmid, pGRP78-luc, and an internal-control plasmid, pRL-TK. The transfected cells were treated with IFN- α (+IFN) from 6 to 36 h posttransfection or left untreated and then further incubated for 6 h in the presence or absence of 1 μ M DMAG. The resulting cells were harvested and subjected to a dual-luciferase assay. The firefly luciferase activity is indicated as the RLU (top) after standardization with that of *Renilla* luciferase. The enhancement of promoter activity by treatment with DMAG is presented as the increase (bottom). (B) Huh7 cells, Huh9-13 cells, and Huh9-13 cells cured by IFN- α treatment (Cured) were cultured for 6 h in the presence or absence of 1 μ M DMAG, and the amount of GRP78 mRNA was measured by real-time PCR. The value of the mRNA was normalized with the amount of GAPDH mRNA (upper left), and the transcriptional enhancement by treatment with DMAG is presented as the increase (lower left). The expression levels of GRP78 and β -actin in the cells were determined by immunoblotting (upper right) and are presented as the increase (lower right). (C) The amounts of GADD153 mRNA in Huh7 cells, Huh9-13 cells, and the cured cells cultured for 6 h in the presence or absence of 1 μ M DMAG were measured by real-time PCR. The values of the mRNA were normalized with the amount of GAPDH mRNA (top), and the transcriptional enhancement by treatment with DMAG is presented as the increase (bottom). The error bars indicate standard deviations. The asterisks indicate significant differences ($P < 0.01$) versus the control value. The data shown are representative of three independent experiments.

ity, while small vesicles show fast movement (68), and FM and EM have revealed that NS5A is colocalized with hB-ind1, as well as FKBP8 (45), in the membranous webs. hB-ind1 was first identified as a regulator of Rac1 that activates JNK and NF- κ B (11). Rac1 is a member of the Rho GTPase family and plays

crucial roles in cytoskeletal dynamics, membrane ruffling, and gene transcription through the effectors of the Rho GTPase family members. IQGAP1 and PAK1 are Rac1 effectors that bind to Rac proteins and are also involved in the replication of HCV (5, 7, 19, 31, 50). The tetratricopeptide repeat domain of immunophilin family members, such as FKBP8, has been shown to interact with Hsp90 (12, 45) and the GR-Hsp90 complex that leads to association with dynein for retrograde transport, along with microtubules (12). Hsp90 has been shown to play an important role in the interaction of transcriptase with genomic RNA of hepatitis B virus (27) and the nuclear transportation of the polymerase of influenza virus (40). Flock house virus also recruits Hsp90 in the polymerase synthesis in the early step of infection (9). Hsp90 may be involved in the regulation of the movement and arrangement of the HCV replication complexes through interaction with Rac1, hB-ind1, and FKBP8. Further investigation is needed to clarify the role of the Hsp90 chaperone system in the life cycle of HCV.

The surrounding membranes, including the membranous web, may protect the viral replication complex and RNA genome against digestion by the host proteases and nucleases (69). The replication complex is composed of viral nonstructural proteins and host proteins, including chaperone and co-chaperone proteins. HCV NS5A has been shown to interact with various host proteins, including cochaperones, such as FKBP8 and hB-ind1, and to recruit a chaperone, Hsp90, into the replication complex through interaction with these cochaperones. Recruitment of the chaperone complex into the replication complex is crucial for the correct folding of newly synthesized viral proteins to maintain the efficient replication of the viral genome. HCV replication has been shown to be improved by the adaptive mutations suppressing the phosphorylation status of NS5A in the replicon cells (3). Although suppression of the hyperphosphorylation of NS5A by treatment with kinase inhibitors improves the replication of the replicons that have no adaptive mutations (42), several kinase inhibitors have been shown to suppress the replication of the HCV replicon carrying the adaptive mutations (29), and phosphorylation of NS5A by casein kinase II was shown to improve virus production but not HCV RNA replication (57). Hsp90 is capable of directly modulating the activities of several kinases (37, 53, 54), and thus, it might be feasible that cochaperones, including hB-ind1 and FKBP8, participate in the propagation of HCV by regulating the phosphorylation status of NS5A in cooperation with Hsp90.

The host chaperone system regulates the quality of client proteins, and impairment of the chaperone activity induces accumulation of misfolded proteins and affects the natural cellular function and viability (20, 21, 33). In this study, DMAG treatment induced a higher level of UPR in HCV replicon cells than in parental and cured cells, indicating that the Hsp90 chaperone system participates in the maintenance of correct folding of the viral and host proteins in the replication complex in the membranous web and in the circumvention of the UPR induced by HCV replication. Treatment with geldanamycin or its derivatives has been shown to inhibit GRP94, which is the Hsp90 paralog located in the ER (10), and to disrupt the ER chaperone pathway, leading to the induction of ER-associated protein degradation, transcriptional attenuation, and eventually induction of apoptosis (34). ER chaperones, such as

GRP94, may also participate in the correct folding of the viral and host proteins in the replication complex for efficient replication of the HCV genome.

Geldanamycin and its derivatives have been reported to remarkably inhibit poliovirus replication *in vivo* without any emergence of drug-resistant escape mutants (22), suggesting that an inhibitor of the chaperone system may be a promising candidate for the treatment of viral infectious diseases with low risk of the emergence of drug-resistant viruses. In addition, Hsp90 inhibitors exhibit anticancer activities through the suppression of various cell signals essential for cancer growth and the enhancement of radiation sensitivity (2, 8, 13). In conclusion, our data indicate that hB-ind1 is included within the HCV replication complex and regulates HCV RNA replication through its own cochaperone activity. Hsp90 and cochaperones, including hB-ind1 and FKBP8, which are required for efficient HCV replication, should be ideal targets for the treatment of chronic hepatitis C with a low frequency of emergence of drug-resistant breakthrough viruses.

ACKNOWLEDGMENTS

We thank H. Murase for her secretarial work. We also thank R. Bartenschlager, T. Wakita, and F. V. Chisari for providing the plasmids and cell lines.

This work was supported in part by grants-in-aid from the Ministry of Health, Labor, and Welfare; the Ministry of Education, Culture, Sports, Science, and Technology; the Global Center of Excellence Program; the Foundation for Biomedical Research and Innovation; and the Naito Foundation.

REFERENCES

- Abe, T., Y. Kaname, I. Hamamoto, Y. Tsuda, X. Wen, S. Tagawa, K. Moriishi, O. Takeuchi, T. Kawai, T. Kanto, N. Hayashi, S. Akira, and Y. Matsuura. 2007. Hepatitis C virus nonstructural protein 5A modulates the toll-like receptor-MyD88-dependent signaling pathway in macrophage cell lines. *J. Virol.* **81**:8953–8966.
- Bisht, K. S., C. M. Bradbury, D. Mattson, A. Kaushal, A. Sowers, S. Markovina, K. L. Ortiz, L. K. Sieck, J. S. Isaacs, M. W. Brechbiel, J. B. Mitchell, L. M. Neckers, and D. Gius. 2003. Geldanamycin and 17-allylamino-17-demethoxygeldanamycin potentiate the *in vitro* and *in vivo* radiation response of cervical tumor cells via the heat shock protein 90-mediated intracellular signaling and cytotoxicity. *Cancer Res.* **63**:8984–8995.
- Blight, K. J., A. A. Kolykhalov, and C. M. Rice. 2000. Efficient initiation of HCV RNA replication in cell culture. *Science* **290**:1972–1974.
- Bohen, S. P., A. Kralli, and K. R. Yamamoto. 1995. Hold 'em and fold 'em: chaperones and signal transduction. *Science* **268**:1303–1304.
- Bost, A. G., D. Venable, L. Liu, and B. A. Heinz. 2003. Cytoskeletal requirements for hepatitis C virus (HCV) RNA synthesis in the HCV replicon cell culture system. *J. Virol.* **77**:4401–4408.
- Brown, G., H. W. Rixon, J. Steel, T. P. McDonald, A. R. Pitt, S. Graham, and R. J. Sugrue. 2005. Evidence for an association between heat shock protein 70 and the respiratory syncytial virus polymerase complex within lipid-raft membranes during virus infection. *Virology* **338**:69–80.
- Bryan, B. A., D. Li, X. Wu, and M. Liu. 2005. The Rho family of small GTPases: crucial regulators of skeletal myogenesis. *Cell Mol. Life Sci.* **62**:1547–1555.
- Calderwood, S. K., M. A. Khaleque, D. B. Sawyer, and D. R. Ciocca. 2006. Heat shock proteins in cancer: chaperones of tumorigenesis. *Trends Biochem. Sci.* **31**:164–172.
- Castorena, K. M., S. A. Weeks, K. A. Stapleford, A. M. Cadwallader, and D. J. Miller. 2007. A functional heat shock protein 90 chaperone is essential for efficient flock house virus RNA polymerase synthesis in *Drosophila* cells. *J. Virol.* **81**:8412–8420.
- Chavany, C., E. Minnaugh, P. Miller, R. Bitton, P. Nguyen, J. Trepel, L. Whitesell, R. Schnur, J. Moyer, and L. Neckers. 1996. p185erbB2 binds to GRP94 *in vivo*. Dissociation of the p185erbB2/GRP94 heterocomplex by benzoquinone ansamycins precedes depletion of p185erbB2. *J. Biol. Chem.* **271**:4974–4977.
- Courilleau, D., E. Chastre, M. Sabbah, G. Redeuilh, A. Atfi, and J. Mester. 2000. B-ind1, a novel mediator of Rac1 signaling cloned from sodium butyrate-treated fibroblasts. *J. Biol. Chem.* **275**:17344–17348.
- Davies, T. H., Y. M. Ning, and E. R. Sanchez. 2002. A new first step in activation of steroid receptors: hormone-induced switching of FKBP51 and FKBP52 immunophilins. *J. Biol. Chem.* **277**:4597–4600.
- Didelot, C., D. Lanneau, M. Brunet, A. L. Joly, A. De Thonel, G. Chiosis, and C. Garrido. 2007. Anti-cancer therapeutic approaches based on intracellular and extracellular heat shock proteins. *Curr. Med. Chem.* **14**:2839–2847.
- Egger, D., B. Wolk, R. Gosert, L. Bianchi, H. E. Blum, D. Moradpour, and K. Bienz. 2002. Expression of hepatitis C virus proteins induces distinct membrane alterations including a candidate viral replication complex. *J. Virol.* **76**:5974–5984.
- Evans, M. J., C. M. Rice, and S. P. Goff. 2004. Genetic interactions between hepatitis C virus replicons. *J. Virol.* **78**:12085–12089.
- Freeman, B. C., S. J. Felts, D. O. Toft, and K. R. Yamamoto. 2000. The p23 molecular chaperones act at a late step in intracellular receptor action to differentially affect ligand efficacies. *Genes Dev.* **14**:422–434.
- Freeman, B. C., and K. R. Yamamoto. 2002. Disassembly of transcriptional regulatory complexes by molecular chaperones. *Science* **296**:2232–2235.
- Frydman, J., and J. Hohfeld. 1997. Chaperones get in touch: the Hip-Hop connection. *Trends Biochem. Sci.* **22**:87–92.
- Fukata, M., M. Nakagawa, and K. Kaibuchi. 2003. Roles of Rho-family GTPases in cell polarisation and directional migration. *Curr. Opin. Cell Biol.* **15**:590–597.
- Garrido, C., M. Brunet, C. Didelot, Y. Zermati, E. Schmitt, and G. Kroemer. 2006. Heat shock proteins 27 and 70: anti-apoptotic proteins with tumorigenic properties. *Cell Cycle* **5**:2592–2601.
- Garrido, C., S. Gurbuxani, L. Ravagnan, and G. Kroemer. 2001. Heat shock proteins: endogenous modulators of apoptotic cell death. *Biochem. Biophys. Res. Commun.* **286**:433–442.
- Geller, R., M. Vignuzzi, R. Andino, and J. Frydman. 2007. Evolutionary restraints on chaperone-mediated folding provide an antiviral approach refractory to development of drug resistance. *Genes Dev.* **21**:195–205.
- Gosert, R., D. Egger, V. Lohmann, R. Bartenschlager, H. E. Blum, K. Bienz, and D. Moradpour. 2003. Identification of the hepatitis C virus RNA replication complex in Huh-7 cells harboring subgenomic replicons. *J. Virol.* **77**:5487–5492.
- Grakoui, A., D. W. McCourt, C. Wychowski, S. M. Feinstone, and C. M. Rice. 1993. Characterization of the hepatitis C virus-encoded serine proteinase: determination of proteinase-dependent polyprotein cleavage sites. *J. Virol.* **67**:2832–2843.
- Hamamoto, I., Y. Nishimura, T. Okamoto, H. Aizaki, M. Liu, Y. Mori, T. Abe, T. Suzuki, M. M. Lai, T. Miyamura, K. Moriishi, and Y. Matsuura. 2005. Human VAP-B is involved in hepatitis C virus replication through interaction with NS5A and NS5B. *J. Virol.* **79**:13473–13482.
- Ho, S. N., H. D. Hunt, R. M. Horton, J. K. Pullen, and L. R. Pease. 1989. Site-directed mutagenesis by overlap extension using the polymerase chain reaction. *Gene* **77**:51–59.
- Hu, J., D. Flores, D. Toft, X. Wang, and D. Nguyen. 2004. Requirement of heat shock protein 90 for human hepatitis B virus reverse transcriptase function. *J. Virol.* **78**:13122–13131.
- Huang, D. C., S. Cory, and A. Strasser. 1997. Bcl-2, Bcl-XL and adenovirus protein E1B19kD are functionally equivalent in their ability to inhibit cell death. *Oncogene* **14**:405–414.
- Huang, Y., K. Staschke, R. De Francesco, and S. L. Tan. 2007. Phosphorylation of hepatitis C virus NS5A nonstructural protein: a new paradigm for phosphorylation-dependent viral RNA replication? *Virology* **364**:1–9.
- Hutchison, K. A., L. F. Stancato, J. K. Owens-Grillo, J. L. Johnson, P. Krishna, D. O. Toft, and W. B. Pratt. 1995. The 23-kDa acidic protein in reticulocyte lysate is the weakly bound component of the hsp foldosome that is required for assembly of the glucocorticoid receptor into a functional heterocomplex with hsp90. *J. Biol. Chem.* **270**:18841–18847.
- Ishida, H., K. Li, M. Yi, and S. M. Lemon. 2007. p21-activated kinase 1 is activated through the mammalian target of rapamycin/p70 S6 kinase pathway and regulates the replication of hepatitis C virus in human hepatoma cells. *J. Biol. Chem.* **282**:11836–11848.
- Kampmueller, K. M., and D. J. Miller. 2005. The cellular chaperone heat shock protein 90 facilitates Flock House virus RNA replication in *Drosophila* cells. *J. Virol.* **79**:6827–6837.
- Kim, H. P., D. Morse, and A. M. Choi. 2006. Heat-shock proteins: new keys to the development of cytoprotective therapies. *Exp. Opin. Ther. Targets* **10**:759–769.
- Lai, E., T. Teodoro, and A. Volchuk. 2007. Endoplasmic reticulum stress: signaling the unfolded protein response. *Physiology* **22**:193–201.
- Lohmann, V., F. Korner, J. Koch, U. Herian, L. Theilmann, and R. Bartenschlager. 1999. Replication of subgenomic hepatitis C virus RNAs in a hepatoma cell line. *Science* **285**:110–113.
- McLauchlan, J., M. K. Lemberg, G. Hope, and B. Martoglio. 2002. Intramembrane proteolysis promotes trafficking of hepatitis C virus core protein to lipid droplets. *EMBO J.* **21**:3980–3988.
- Miyata, Y., and I. Yahara. 1992. The 90-kDa heat shock protein, HSP90, binds and protects casein kinase II from self-aggregation and enhances its kinase activity. *J. Biol. Chem.* **267**:7042–7047.
- Momose, F., T. Naito, K. Yano, S. Sugimoto, Y. Morikawa, and K. Nagata.

2002. Identification of Hsp90 as a stimulatory host factor involved in influenza virus RNA synthesis. *J. Biol. Chem.* **277**:45306–45314.
39. **Moradpour, D., F. Penin, and C. M. Rice.** 2007. Replication of hepatitis C virus. *Nat. Rev. Microbiol.* **5**:453–463.
40. **Naito, T., F. Momose, A. Kawaguchi, and K. Nagata.** 2007. Involvement of Hsp90 in assembly and nuclear import of influenza virus RNA polymerase subunits. *J. Virol.* **81**:1339–1349.
41. **Neckers, L.** 2002. Hsp90 inhibitors as novel cancer chemotherapeutic agents. *Trends Mol. Med.* **8**:S55–S61.
42. **Neddermann, P., M. Quintavalle, C. Di Pietro, A. Clementi, M. Cerretani, S. Altamura, L. Bartholomew, and R. De Francesco.** 2004. Reduction of hepatitis C virus NS5A hyperphosphorylation by selective inhibition of cellular kinases activates viral RNA replication in cell culture. *J. Virol.* **78**:13306–13314.
43. **Okamoto, K., Y. Mori, Y. Komoda, T. Okamoto, M. Okochi, M. Takeda, T. Suzuki, K. Moriishi, and Y. Matsuura.** 2008. Intramembrane processing by signal peptide peptidase regulates the membrane localization of hepatitis C virus core protein and viral propagation. *J. Virol.* **82**:8349–8361.
44. **Okamoto, K., K. Moriishi, T. Miyamura, and Y. Matsuura.** 2004. Intramembrane proteolysis and endoplasmic reticulum retention of hepatitis C virus core protein. *J. Virol.* **78**:6370–6380.
45. **Okamoto, T., Y. Nishimura, T. Ichimura, K. Suzuki, T. Miyamura, T. Suzuki, K. Moriishi, and Y. Matsuura.** 2006. Hepatitis C virus RNA replication is regulated by FKBP8 and Hsp90. *EMBO J.* **25**:5015–5025.
46. **Okamoto, T., H. Omori, Y. Kaname, T. Abe, Y. Nishimura, T. Suzuki, T. Miyamura, T. Yoshimori, K. Moriishi, and Y. Matsuura.** 2008. A single-amino-acid mutation in hepatitis C virus NS5A disrupting FKBP8 interaction impairs viral replication. *J. Virol.* **82**:3480–3489.
47. **Pietschmann, T., V. Lohmann, A. Kaul, N. Krieger, G. Rinck, G. Rutter, D. Strand, and R. Bartenschlager.** 2002. Persistent and transient replication of full-length hepatitis C virus genomes in cell culture. *J. Virol.* **76**:4008–4021.
48. **Prapapanich, V., S. Chen, E. J. Toran, R. A. Rimerman, and D. F. Smith.** 1996. Mutational analysis of the hsp70-interacting protein Hip. *Mol. Cell. Biol.* **16**:6200–6207.
49. **Pratt, W. B., and D. O. Toff.** 1997. Steroid receptor interactions with heat shock protein and immunophilin chaperones. *Endocr. Rev.* **18**:306–360.
50. **Ridley, A. J., H. F. Paterson, C. L. Johnston, D. Diekmann, and A. Hall.** 1992. The small GTP-binding protein rac regulates growth factor-induced membrane ruffling. *Cell* **70**:401–410.
51. **Rieder, C. L., and S. S. Bowser.** 1985. Correlative immunofluorescence and electron microscopy on the same section of epon-embedded material. *J. Histochem. Cytochem.* **33**:165–171.
52. **Sanchez, E. R., D. O. Toff, M. J. Schlesinger, and W. B. Pratt.** 1985. Evidence that the 90-kDa phosphoprotein associated with the untransformed L-cell glucocorticoid receptor is a murine heat shock protein. *J. Biol. Chem.* **260**:12398–12401.
53. **Sato, S., N. Fujita, and T. Tsuruo.** 2000. Modulation of Akt kinase activity by binding to Hsp90. *Proc. Natl. Acad. Sci. USA* **97**:10832–10837.
54. **Stancato, L. F., A. M. Silverstein, J. K. Owens-Grillo, Y. H. Chow, R. Jove, and W. B. Pratt.** 1997. The hsp90-binding antibiotic geldanamycin decreases Raf levels and epidermal growth factor signaling without disrupting formation of signaling complexes or reducing the specific enzymatic activity of Raf kinase. *J. Biol. Chem.* **272**:4013–4020.
55. **Stravopodis, D. J., L. H. Margaritis, and G. E. Voutsinas.** 2007. Drug-mediated targeted disruption of multiple protein activities through functional inhibition of the Hsp90 chaperone complex. *Curr. Med. Chem.* **14**:3122–3138.
56. **Taguwa, S., T. Okamoto, T. Abe, Y. Mori, T. Suzuki, K. Moriishi, and Y. Matsuura.** 2008. Human butyrate-induced transcript 1 interacts with hepatitis C virus NS5A and regulates viral replication. *J. Virol.* **82**:2631–2641.
57. **Tellinghuisen, T. L., K. L. Foss, and J. Treadaway.** 2008. Regulation of hepatitis C virion production via phosphorylation of the NS5A protein. *PLoS Pathog.* **4**:e1000032.
58. **Tellinghuisen, T. L., J. Marcotrigiano, and C. M. Rice.** 2005. Structure of the zinc-binding domain of an essential component of the hepatitis C virus replicase. *Nature* **435**:374–379.
59. **Terasawa, K., M. Minami, and Y. Minami.** 2005. Constantly updated knowledge of Hsp90. *J. Biochem.* **137**:443–447.
60. **Tomei, L., C. Failla, E. Santolini, R. De Francesco, and N. La Monica.** 1993. NS3 is a serine protease required for processing of hepatitis C virus polyprotein. *J. Virol.* **67**:4017–4026.
61. **Tu, H., L. Gao, S. T. Shi, D. R. Taylor, T. Yang, A. K. Mircheff, Y. Wen, A. E. Gorbalenya, S. B. Hwang, and M. M. Lai.** 1999. Hepatitis C virus RNA polymerase and NS5A complex with a SNARE-like protein. *Virology* **263**:30–41.
62. **Wakita, T., T. Pietschmann, T. Kato, T. Date, M. Miyamoto, Z. Zhao, K. Murthy, A. Habermann, H. G. Krausslich, M. Mizokami, R. Bartenschlager, and T. J. Liang.** 2005. Production of infectious hepatitis C virus in tissue culture from a cloned viral genome. *Nat. Med.* **11**:791–796.
63. **Wang, C., M. Gale, Jr., B. C. Keller, H. Huang, M. S. Brown, J. L. Goldstein, and J. Ye.** 2005. Identification of FBL2 as a geranylgeranylated cellular protein required for hepatitis C virus RNA replication. *Mol. Cell* **18**:425–434.
64. **Wasley, A., and M. J. Alter.** 2000. Epidemiology of hepatitis C: geographic differences and temporal trends. *Semin. Liver Dis.* **20**:1–16.
65. **Watahi, K., N. Ishii, M. Hijikata, D. Inoue, T. Murata, Y. Miyanari, and K. Shimotohno.** 2005. Cyclophilin B is a functional regulator of hepatitis C virus RNA polymerase. *Mol. Cell* **19**:111–122.
66. **Whitesell, L., and S. L. Lindquist.** 2005. HSP90 and the chaperoning of cancer. *Nat. Rev. Cancer.* **5**:761–772.
67. **Wochnik, G. M., J. C. Young, U. Schmidt, F. Holsboer, F. U. Hartl, and T. Rein.** 2004. Inhibition of GR-mediated transcription by p23 requires interaction with Hsp90. *FEBS Lett.* **560**:35–38.
68. **Wolk, B., B. Buchele, D. Moradpour, and C. M. Rice.** 2008. A dynamic view of hepatitis C virus replication complexes. *J. Virol.* **82**:10519–10531.
69. **Yang, G., D. C. Pevear, M. S. Collett, S. Chunduru, D. C. Young, C. Benetatos, and R. Jordan.** 2004. Newly synthesized hepatitis C virus replicon RNA is protected from nuclease activity by a protease-sensitive factor(s). *J. Virol.* **78**:10202–10205.
70. **Zhong, J., P. Gastaminza, G. Cheng, S. Kapadia, T. Kato, D. R. Burton, S. F. Wieland, S. L. Uprichard, T. Wakita, and F. V. Chisari.** 2005. Robust hepatitis C virus infection in vitro. *Proc. Natl. Acad. Sci. USA* **102**:9294–9299.

Human VAP-C Negatively Regulates Hepatitis C Virus Propagation[∇]

Hiroshi Kukihara,¹ Kohji Moriishi,¹ Shuhei Taguwa,¹ Hideki Tani,¹ Takayuki Abe,¹
Yoshio Mori,¹ Tetsuro Suzuki,² Takasuke Fukuhara,^{1,3} Akinobu Taketomi,³
Yoshihiko Maehara,³ and Yoshiharu Matsuura^{1*}

Department of Molecular Virology, Research Institute for Microbial Diseases, Osaka University, Osaka,¹ Department of Virology II, National Institute of Infectious Diseases, Tokyo,² and Department of Surgery and Science, Graduate School of Medical Sciences, Kyushu University, Fukuoka,³ Japan

Received 3 May 2009/Accepted 2 June 2009

Human vesicle-associated membrane protein-associated protein (VAP) subtype A (VAP-A) and subtype B (VAP-B) are involved in the regulation of membrane trafficking, lipid transport and metabolism, and the unfolded protein response. VAP-A and VAP-B consist of the major sperm protein (MSP) domain, the coiled-coil motif, and the C-terminal transmembrane anchor and form homo- and heterodimers through the transmembrane domain. VAP-A and VAP-B interact with NS5B and NS5A of hepatitis C virus (HCV) through the MSP domain and the coiled-coil motif, respectively, and participate in the replication of HCV. VAP-C is a splicing variant of VAP-B consisting of the N-terminal half of the MSP domain of VAP-B followed by the subtype-specific frameshift sequences, and its biological function has not been well characterized. In this study, we have examined the biological functions of VAP-C in the propagation of HCV. VAP-C interacted with NS5B but not with VAP-A, VAP-B, or NS5A in immunoprecipitation analyses, and the expression of VAP-C inhibited the interaction of NS5B with VAP-A or VAP-B. Overexpression of VAP-C impaired the RNA replication of the HCV replicon and the propagation of the HCV JFH1 strain, whereas overexpression of VAP-A and VAP-B enhanced the replication. Furthermore, the expression of VAP-C was observed in various tissues, whereas it was barely detected in the liver. These results suggest that VAP-C acts as a negative regulator of HCV propagation and that the expression of VAP-C may participate in the determination of tissue tropism of HCV propagation.

Hepatitis C virus (HCV) is a major causative agent of chronic liver disease and thus a major public health problem, infecting at least 3% of the world population (47). HCV infection proceeds to the persistent stage in approximately 80% of patients, leading to the development of cirrhosis in 20% to 50% of patients, of whom approximately 5% eventually develop hepatocellular carcinoma (12). HCV encompasses a single-stranded positive-sense RNA genome of approximately 9.6 kb, which encodes a large precursor polyprotein comprising approximately 3,000 amino acids (26). The structural proteins are cleaved from the N-terminal one-fourth of the polyprotein by the host signal peptidase and signal peptide peptidase (23, 32, 33), resulting in the maturation of the capsid protein, two envelope proteins and viroporin p7. The NS2 protease cleaves after the carboxyl terminus, and then NS3 cleaves the appropriate downstream positions to produce NS4A, NS4B, NS5A, and NS5B (8, 42), all of which form the replication complex along with several host proteins (5, 21). NS5B is the RNA-dependent RNA polymerase, which is a main enzymatic component of the replication complex of HCV (3), while NS5A is a membrane-anchored zinc-binding phosphoprotein that appears to possess diverse functions, including the suppression of host defense and the regulation of the virus's replication (1, 4, 6, 41), although its biological function remains unclear.

The NS5A protein has been shown to interact with several host proteins, including vesicle-associated membrane protein (VAMP)-associated protein (VAP) subtype A (VAP-A) (44) and subtype B (VAP-B) (9), FKBP8 (34), MyD88 (1), FBL2 (46), human butyrate-induced transcript 1 (hB-ind1) (40), and so on (25). VAP-A and VAP-B also bind to NS5B, although it remains unclear whether these interactions modulate HCV replication positively or negatively (9, 44). VAP-A and VAP-B have been shown to associate with the cytoplasmic face of the endoplasmic reticulum (ER) and the Golgi apparatus (38) and to consist of the major sperm protein (MSP) domain, the coiled-coil domain, and the transmembrane (TM) region, in that order (30, 39), as shown in Fig. 1A. VAP was originally reported as a protein binding to VAMP, which is a synaptic vesicle SNARE protein required for synaptic-vesicle fusion in the nematode *Aplysia californica*, and was designated the 33-kDa VAMP-associated protein, VAP-33 (39). Two mammalian homologues, VAP-A and VAP-B, were subsequently identified (30, 38). The transcription of VAP-A and VAP-B is ubiquitously detected in mammalian organs, including the heart, placenta, lung, liver, skeletal muscle, and pancreas (30), suggesting that VAP family proteins are involved in diverse cellular functions other than neurotransmitter release (30, 38, 49). Several VAP-interacting proteins share the FFAT motif (two phenylalanines in an acidic tract), which has the consensus amino acid sequence EFFDAXE, as determined by a comparison among oxysterol binding proteins (OSBPs), OSBP-related proteins (ORPs) (20), and the ceramide transport protein CERT (10, 19), contributing to the regulation of fatty acid metabolism. The interaction of VAP family proteins with

* Corresponding author. Mailing address: Department of Molecular Virology, Research Institute for Microbial Diseases, Osaka University, 3-1, Yamadaoka, Suita, Osaka 565-0871, Japan. Phone: 81-6-6879-8340. Fax: 81-6-6879-8269. E-mail: matsuura@biken.osaka-u.ac.jp.

[∇] Published ahead of print on 10 June 2009.